



HAL
open science

Cell wall polysaccharides, phenolic extractability and mechanical properties of Aleatico winegrapes dehydrated under sun or in controlled conditions

Giulia Scalzini, Aude Vernhet, Stéphanie Carillo, Stéphanie Roi, Frédéric Véran, Bodil Jørgensen, Jeanett Hansen, Simone Giacosa, Susana Río Segade, Maria Alessandra Paissoni, et al.

► To cite this version:

Giulia Scalzini, Aude Vernhet, Stéphanie Carillo, Stéphanie Roi, Frédéric Véran, et al.. Cell wall polysaccharides, phenolic extractability and mechanical properties of Aleatico winegrapes dehydrated under sun or in controlled conditions. *Food Hydrocolloids*, 2024, 149, pp.109605. 10.1016/j.foodhyd.2023.109605 . hal-04575978

HAL Id: hal-04575978

<https://hal.inrae.fr/hal-04575978>

Submitted on 15 May 2024

HAL is a multi-disciplinary open access archive for the deposit and dissemination of scientific research documents, whether they are published or not. The documents may come from teaching and research institutions in France or abroad, or from public or private research centers.

L'archive ouverte pluridisciplinaire **HAL**, est destinée au dépôt et à la diffusion de documents scientifiques de niveau recherche, publiés ou non, émanant des établissements d'enseignement et de recherche français ou étrangers, des laboratoires publics ou privés.

Copyright



Cell wall polysaccharides, phenolic extractability and mechanical properties of Aleatico winegrapes dehydrated under sun or in controlled conditions

Giulia Scalzini^a, Aude Vernhet^b, Stéphanie Carillo^b, Stéphanie Roi^b, Frédéric Véran^b, Bodil Jørgensen^c, Jeanett Hansen^c, Simone Giacosa^a, Susana Ríó Segade^a, Maria Alessandra Paissoni^a, Thierry Doco^{b,***}, Luca Rolle^{a,*}, Céline Poncet-Legrand^{b,**}

^a Department of Agricultural, Forest and Food Sciences, University of Torino, Corso Enotria 2/C, 12051, Alba, Italy

^b SPO - University of Montpellier, INRAE, Institut Agro Montpellier Supagro, 34070, Montpellier, France

^c Department of Plant and Environmental Sciences, University of Copenhagen, Thorvaldsensvej 40, 1871, Frederiksberg C, Denmark

ARTICLE INFO

Keywords:

Grape dehydration
Postharvest withering
Aleatico
Polysaccharides
Phenolic extractability

ABSTRACT

Aleatico is an Italian red winegrape variety traditionally used partially dehydrated to produce Passito wines. The aim of this research is to assess the effect of two different off-vine withering techniques (natural sun-exposed: SUN, and controlled temperature and humidity conditions: CTR) on grapes physicochemical modifications, focusing on mechanical properties, phenolic profile, and cell-wall polysaccharide structures. The composition and extractability of polyphenols were studied before and after the two withering processes, differentiating the tissues (skin, pulp, seeds). A stronger effect on cell-wall polysaccharides composition pectin was highlighted by chemical and immunochemical approaches in SUN skins at the level of pectin chains and de-esterification, affecting grapes mechanical properties, especially for skin rigidity ($<E_{sk}$). Sun-dehydrated grapes showed the highest pH (about 0.3 units more than FRESH and CTR), and the lowest acidity (-0.71 g/L vs FRESH) and anthocyanin content in wine-like solution (-41%), whereas these parameters were better preserved in controlled conditions. Instead, seeds tannins were higher in SUN than other samples, with a lower oligomers/polymers ratio. Indeed, after withering the phenolic extractability decreased in skins (total phenolics: from 60% for FRESH to 40% for SUN; anthocyanins: from 72% for FRESH to 46% for SUN) and increased in seeds (total phenolics: from 30% for FRESH to 41% for SUN) compared with fresh samples, in both cases more markedly for SUN than CTR. Skin phenolic composition after 10 days of simulated-maceration was affected by the combination of the loss/concentration balance, together with their modified release in the wine-like solution. As regards seeds, instead, the differences highlighted by the extractable profiles were due to the modified extractability as consequence of the different withering conditions and not to chemical quantitative/qualitative modifications of phenolic compounds caused by dehydration.

1. Introduction

The postharvest withering of winegrapes is an important practice in winemaking, which consists in a partial dehydration of the grapes after the harvest inducing metabolic changes that modify their physical and chemical features. The special sweet wines produced with withered grapes have generally unique characteristics, which are improving their

territorial identity and commercial values (Sanmartin et al., 2021).

Among wines produced with withered grapes, sweet red wines are very complex because they are rich in phenolic compounds that strongly influence their sensory features (Marquez, Serratos, Lopez-Toledano, & Merida, 2014). The main classes of phenolic compounds include anthocyanins, which are present in the berry skins and determine the color traits of wine, flavan-3-ols, oligomeric, and polymeric tannins from both

* Corresponding author.

** Corresponding author.

*** Corresponding author.

E-mail addresses: luca.rolle@unito.it (L. Rolle), celine.poncet-legrand@inrae.fr (C. Poncet-Legrand).

<https://doi.org/10.1016/j.foodhyd.2023.109605>

Received 17 August 2023; Received in revised form 23 November 2023; Accepted 28 November 2023

Available online 6 December 2023

0268-005X/© 2023 The Author(s). Published by Elsevier Ltd. This is an open access article under the CC BY license (<http://creativecommons.org/licenses/by/4.0/>).

skins and seeds, responsible for bitterness and astringency, and other class of compounds involved in many crucial reactions such as phenolic acids (Chira, Schmauch, Saucier, Fabre, & Teissedre, 2009; Scalzini, Giacosa, Río Segade, Pissoni, & Rolle, 2021).

During the withering process, a loss of water in the berries occurs, leading to grape weight loss from relatively low values of 20–30%, reached for most wines, to the highest 40–50% such as for Passito di Pantelleria wines or up to 50% for certain Pedro Ximenez sweet Sherry wines. This phenomenon causes the concentration of primary and secondary metabolites (Corona et al., 2020; Sanmartin et al., 2021). At the same time, catabolism and oxidation reactions also take place because of the natural senescence of grape berry tissues and of the stress caused by water evaporation that enhances continuously the concentration gradient (Mencarelli & Bellincontro, 2013). Therefore, the final concentration of grape quality markers, such as sugars, acidity, and phenolic compounds, is the result of a composite balance between (i) concentration and synthesis of metabolites and (ii) loss of compounds caused by oxidation and catabolism (Bonghi et al., 2012; De Rosso et al., 2016). The dehydration kinetics and berry metabolism modifications strongly depend on the withering conditions (i.e. temperature, relative humidity, and air flow speed) and genetic features of grape variety, such as the skin thickness and the ability to activate different genetic responses (Rolle, Torchio, Giacosa, & Gerbi, 2009; Zenoni et al., 2016). Moreover, under the same environmental conditions, specific classes of phenolic compounds are differently affected by the dehydration process (Toffali et al., 2011).

Another important aspect that needs to be considered is the different extraction kinetics and yield of the compounds present in grapes, being the extractability of phenolic compounds strongly influenced by the cell wall structure and composition. Indeed, it is influenced by cell wall porosity, as well as the binding of polyphenols with cell wall proteins and polysaccharides, and by the modifications of mechanical features induced by their rearrangements (Bindon, Madani, Pendleton, Smith, & Kennedy, 2014; Hanlin, Hrmova, Harbertson, & Downey, 2010; Río Segade, Pissoni, Giacosa, et al., 2019). Therefore, in addition to the challenge of studying the complex metabolic modifications during withering, there is the added difficulty of the change of extractability due to the adaptation of grape berry tissues to dehydration. Many studies have focused on the chemical modification of phenolic compounds during dehydration (Figueiredo-González, Cancho-Grande, & Simal-Gándara, 2013), but very few ones were specifically dedicated to the effect of the modified extractability from the different parts of the grape berry, especially for seeds (Río Segade et al., 2016). Fasoli et al. (2019) highlighted a detailed understanding of cell wall biochemical changes and polysaccharide rearrangements during withering in the skins of grapes cv. Corvina. Nevertheless, Zoccatelli et al. (2013) pointed out that postharvest withering affects pectin metabolism in a cultivar-specific way related to the kinetic of the water loss. Moreover, no study has been performed until now on the influence of different withering conditions on the polysaccharide composition of dehydrated grapes, despite the great importance for the extractability of phenolic compounds, and a complete understanding is still missing.

In the present study, two withering systems were assessed on Aleatico grapes: sun-dehydration practice and withering technique under controlled conditions. The aim was to examine the effect of these two very different withering modalities on the potential and extractable phenolic profile of Aleatico winegrapes. The expected contribution is to provide new insights in the understanding of the modified extractability of phenolic compounds from the distinct parts of grapes subjected to very different withering conditions mainly on the basis of the cell wall polysaccharide composition. It will allow to add new awareness to the comprehension of the withering complexity both from a chemical and a practical winemaking point of view.

Aleatico (*Vitis vinifera* L.) was chosen, as a typical Italian winegrape variety with peculiar polyphenolic features, which are strongly affected by the withering technique. Indeed, Aleatico grapes are rich in phenolic

compounds, but with a low anthocyanin content, characterized by an anthocyanin profile majority constituted of tri-substituted forms (i.e. with three substituents on the lateral B ring; Bellincontro, Fardelli, De Santis, Botondi, & Mencarelli, 2006; Tuccio, 2011). Indeed, Aleatico is an aromatic red variety traditionally used to produce high-quality sweet wines from postharvest withered grapes (Frangipane, Torresi, De Santis, & Massantini, 2012; Mencarelli et al., 2010). It is mainly cultivated in the warm area of central and southern Italy, but it is also present with a few hectares planted in France (Corse), Malta, USA (California), Chile, Australia, and in the central Asian countries of Kazakhstan and Uzbekistan, due to its tolerance to poor soils and water stress conditions (Anderson & Aryal, 2013, p. 700; Tuccio, 2011). Traditionally, on the Elba Island, one of the regions where Aleatico is most widespread and historically produced, the postharvest dehydration occurs under the sun, covering the grapes overnight to protect them from dew. More recently, the withering technique under controlled conditions has spread (Frangipane et al., 2012).

2. Materials and methods

2.1. Grape materials and withering process conditions

In 2021, about 100 kg of Aleatico red winegrapes (*Vitis vinifera* L.) were harvested at technological maturity (historically 24–25 °Brix, pH 3.25–3.35, 5.5–6.0 g/L of titratable acidity expressed as tartaric acid) from ten-years-old grapevines in a commercial vineyard managed with organic cultural practices and located in Castagneto Carducci (Tuscany, Italy, latitude 43°09.936' and longitude 10°37.845', altitude 200 m above sea level).

Once harvested on September 15, 2021, a grape sample of 5 kg was randomly collected for the analysis of fresh material before withering (fresh sample, FRESH). Then, the remaining 100 kg of grape bunches were placed on 40 single-layer IP/4615/UVA perforated plastic crates (400 × 600 × 15 h mm, about 2.5 kg of whole bunch clusters each; Plastic Boxes Srl, Castagnaro (VR), Italy).

Twenty perforated boxes were placed in a dehydration room under controlled conditions (controlled withering, CTR) at about 22 °C, 60% relative humidity (RH) and 1.5 m/s air flow speed. At the same time, the other 20 boxes were exposed to the sun and covered with plastic panels during the night to protect them from dew during the withering period (sun withering, SUN). Thermo-hygrometric withering conditions were measured using a Temperature and Humidity Smart Sensor IBS-TH1 (−40–100 °C ± 0.5 °C, 0–100% ± 6% RH, Inkbird Tech. C.L., Shenzhen, Hong Kong, China). Air flow speed in the controlled dehydration room was measured with the aid of a Mini Anemometer UT363BT (0–30 m/s ± 0.1 m/s, Uni-Trend Technology, China).

The weight loss percentage (WL%) was calculated as $[1 - (\text{net weight of withered grapes in kg} / \text{net weight of fresh grapes in kg})]$ using the weight data measured with a ODECA ACS-30Z precision electronic balance with a maximum weight capacity of 30 kg ± 1 g (Odeca Srl, Varese, Italy). For each withering method, the initial weight of eight sample boxes marked with a code was compared with the weight periodically measured for the same crates. The CTR and SUN samples were withered until reaching the 30% WL each.

2.2. Sample preparation and grape must technological parameters

For each sample (FRESH, and SUN and CTR at 30% WL), the berries were carefully separated from the stalk, cutting them near to the pedicel, and visually inspected to eliminate the damaged ones. Then, three replicates of 150 g of berries for each treatment studied were randomly collected and manually crushed. The musts obtained were centrifuged at 4500 rpm for 15 min at 20 °C in a Hettich 32R centrifuge (Tuttligen, Germany) for the determination of technological parameters. An aliquot of supernatant has been used to evaluate pH by potentiometry with an InoLab 730 pHmeter (WTW, Weilheim, Germany), titratable acidity (as

g/L of tartaric acid) by titration with sodium hydroxide 0,1 N, according to OIV-MA-AS313-01 method (OIV, 2021), and total soluble solids ($^{\circ}$ Brix) using a Atago Palette 0–32 refractometer with automatic temperature compensation (Atago Corporation, Tokyo, Japan).

2.3. Evaluation of berry mechanical properties

Two sets of 40 berries were randomly collected for each sample (FRESH, SUN, and CTR), and individually subjected to the texture tests (i.e. puncture, compression, and traction test). Grape mechanical properties were evaluated using a TA.XTplus Universal Texture Machine (Stable Micro Systems, Godalming, Surrey, United Kingdom) equipped with a 5 kg load cell and an HPD/90 platform. Stable Micro Systems probes have been mounted on the instrument, according to the test to be performed. In particular, a SMS P/2N needle probe (\varnothing 2 mm) was used for the puncture test, a flat probe (P/2 \varnothing 2 mm) for the compression test, and an A/PS probe modified with a rigid arm for the traction test, in order to evaluate the skin hardness (F_{sk} , maximum break force, N; W_{sk} , break energy, mJ), skin resistance to the axial deformation (E_{sk}), skin thickness (Sp_{sk} , μ m), and the peduncle detachment resistance (F_{ped} , N; W_{ped} , mJ), respectively. For the tests concerning grape skins, the skins were manually peeled using a laboratory spatula, and the skins were immediately analyzed by the Universal Texture Machine. The conditions applied were the same as described by Giacosa et al. (2019).

The data were acquired and analyzed using the Texture Exponent software (Stable Micro Systems).

2.4. Extraction of potential and extractable phenolic compounds

To evaluate the extractability of phenolic compounds, two different extraction methods were performed.

A simulated maceration was conducted separately for skins and seeds to evaluate the extractable phenolic profile of the two components in wine-like conditions (EXT). To achieve this goal, a wine-like buffer solution without ethanol was prepared (pH 3.5, 5 g/L tartaric acid, 100 mg/L sodium metabisulphite). For each sample (FRESH, SUN and CTR), three replicates of 80 g of berries each were weighed and manually peeled with the aid of a laboratory spatula. Skins and seeds were carefully separated, cleaned from the flesh, and each component was immediately immersed in 100 mL of buffer solution, in accordance with the liquid-to-solid ratio estimated by Mattivi, Zulian, Nicolini, and Valenti (2002). To simulate the red wine fermentation, skins and seeds were macerated separately throughout 10 days at 25 $^{\circ}$ C with stepwise addition of absolute ethanol at 24, 48, 96, 144, and 192 h of maceration to reach at the final point an ethanol concentration of 15% v/v (2, 2, 4, 4, and 3% v/v of ethanol addition, respectively for each point). Every day, the extracts were homogenized twice with a magnetic stirring bar (20×6 mm) contained in each flask. Before each addition, an equal aliquot of extract sample was taken to maintain constant the volume of the macerating solution. The aliquots were used to study the extraction kinetics of anthocyanins, color, and total polyphenols. At the end of the simulated macerations (10 days), the whole liquid extracts were collected to investigate thoroughly their phenolic profile. The results were expressed as mg/g of skins or seeds using the respective weight of skins and seeds for each replicate, or as mg/kg of berries using the relative grape weight for each sample.

To extract the phenolic compounds potentially present in the grapes (POT), three sets of 30 berries for each sample (FRESH, SUN, CTR) were randomly selected, weighed, and treated following the method described by *Abi-Habib et al.* (2021). Frozen skins, seeds, and flesh were gently ground to a fine powder in a liquid nitrogen mill with the aid of a Pulvérisette 2 mortar grinder (10–20 μ m final finesses, 6–8 mm feed size, FRITTSCH, Idar-Oberstein, Germany). 150 mg of frozen skins powder or 100 mg of frozen seeds powder were treated with 750 μ L of methanol, then added with 5.25 mL of acetone/water/formic acid extraction solvent (60:40:1 v/v). In the case of the flesh, 100 mg of flesh

powder were added with 600 μ L of methanol and 3.4 mL of the extraction solvent. 10 marbles (\varnothing 11 mm) were added in each tube to stir the solution during the extraction-homogenization phase, which was performed at 20 $^{\circ}$ C using a Precellys 24 orbital shaker (Bertin Technologies, Saint-Aubin, France). Then, the extracts were centrifuged at 4 $^{\circ}$ C (1030 \times g for 5 min for skins, 2790 \times g for 5 min for the flesh, and 4140 \times g for 15 min for seeds) in a Hettich 4–16 KS centrifuge (Tuttingen, Germany). The supernatant of each sample was redistributed in 1 mL aliquots and dried under vacuum at 35 $^{\circ}$ C for 2 h in an EZ-2 plus Genevac rotatory evaporator (Warminster, USA). For every replicate of each sample, the extraction was performed in three sub-replicates, to avoid adding variability due to the extraction phase. The dried extracts were redissolved in a wine-like solution (15% v/v, 5 g/L tartaric acid, pH 3.5, and 100 mg/L sodium metabisulphite) for UV–visible spectrophotometry analysis, a water/methanol/formic acid solution (50:50:1 v/v) for HPLC, or dimethyl formamide for High Performance Size Exclusion Chromatography (HPSEC) analysis.

2.5. Phenolic compounds analysis

Total anthocyanin Index (TAnI), total phenolic index (TPI), condensed tannins (or proanthocyanidins, CT) and low molecular weight flavanols (vanillin assay or FRV) were determined by UV–visible spectrophotometry methods (Petrozziello et al., 2018) with a UV-1800 spectrophotometer (Shimadzu Corp., Kyoto, Japan). TAnI (mg of malvidin-3-O-glucoside per kg of grape berries or g of skins) and TPI (mg of (–)-epicatechin per kg of grape berries, g of skins or g of seeds) were evaluated at 536–540 and 280 nm by diluting the sample with an ethanol/water/37% hydrochloric acid solution (70:30:1 v/v) and water, respectively. CT (mg of (–)-epicatechin per kg of grapes, g of skins or g of seeds) were quantified by methyl cellulose precipitation assay according to *Sarneckis et al.* (2006) method. FRV (mg of (+)-catechin/kg of grape berries, g of skins or g of seeds) were determined using the method reported by *Torchio, Cagnasso, Gerbi, and Rolle* (2010).

Anthocyanin profile and phenolic acids were analyzed by HPLC using a Waters HPLC-DAD system and a reversed-phase dC18 column Atlantis T3 (2,1 \times 250 mm i.d.) with a guard column of the same material (Waters Corporation, Milford, USA). The samples were directly injected (5 μ L), with a flow rate of 0.25 mL/min at 30 $^{\circ}$ C. The mobile phase consisted of A = formic acid/water (5:95 v/v) and B = acetonitrile/water/formic acid (80:15:5 v/v). Proportions of solvent B work in gradient mode from 0% for 5 min, increased up to 10% in 30 min, to 20% in 30 min, and to 100% in 5 min (*Fournand et al.*, 2006). Individual anthocyanins were quantified at 520 nm (malvidin-3-O-glucoside equivalents) and phenolic acids at 320 nm (caftaric and coumaric acid equivalents).

The size distribution of polymeric tannins was determined by high pressure size exclusion chromatography (HPSEC) using an Agilent 1260 HPLC system (Santa Clara, California, USA), equipped with 3 PLgel columns (Phenomenex, Torrance, California, USA) composed of highly cross-linked polystyrene-divinylbenzene (300 \times 7.8 mm, 5 μ m, 50 and 100 Å pore size, respectively) and connected in series with a guard column of the same material, according to the method described by *Vernhet et al.* (2020). The mobile phase (DMF) was composed of dimethylformamide, 1% v/v glacial acetic acid, 5% v/v water, and 0.15 M lithium chloride. The flow rate was 0.8 mL/min and the column temperature was 60 $^{\circ}$ C. The columns were calibrated using commercial standards (ellagic acid, catechin, epicatechin, dimer B2, and trimer C1) as well as tannins fractions of different DP (degree of polymerization, the number of flavanol units in a compound), and fractions of anthocyanins purified in the laboratory (*Gomez et al.*, 2009; *Vernhet, Carrillo, & Poncet-Legrand*, 2014). These injections allow to perform an epicatechin equivalent quantification and DP estimation on the different samples using the calibration curve to evaluate the molar mass of tannins as a function of the retention time according to the relationship $\log(M_w) = f(Rt)$.

2.6. Color features determination

The color study of the skin extracts was carried out following the OIV methods (2021). In particular, the visible spectra (380–780 nm) of the undiluted samples were acquired at each maceration sampling point and at the end of the simulated maceration for each of the three biological replicates for FRESH, SUN and CTR, using 1 mm optical path cuvettes. CIEL*a*b parameters, namely lightness (L^*), red/green color coordinate (a^*), and yellow/blue color coordinate (b^*), were calculated following the OIV-MA-AS2-11 method. The color difference between control and treated samples (ΔE^*) was calculated following the relationship $\Delta E^* = [(\Delta L^*)^2 + (\Delta a^*)^2 + (\Delta b^*)^2]^{1/2}$. Color intensity ($A_{420\text{ nm}} + A_{520\text{ nm}} + A_{620\text{ nm}}$, calculated on an optical path of 10 mm) and tonality ($A_{420\text{ nm}}/A_{520\text{ nm}}$) were evaluated according to the OIV-MA-AS2-07B method.

2.7. Preparation of alcohol-insoluble skin cell wall material

The alcohol insoluble solids (AISs) were isolated from the frozen skins and flesh powders according to the procedure described by Apolinar-Valiente, Romero-Cascales, Gómez-Plaza, López-Roca, and Ros-García (2015), applying the modifications adopted by Abi-Habib et al. (2021). For each sample replicate (three for FRESH, SUN and CTR), 5 g of frozen skins powder or 10 g of frozen flesh powder were suspended in 15 mL of boiling water for 5 min and homogenized with a magnetic stirrer to inactivate the enzymes. One part of the homogenized material was mixed with two parts of 96% ethanol for 30 min at 40 °C in a Polystat I 33194 220V heating circulator (Fisher Bioblock Scientific s.a., Illkirch, France). The AISs were centrifuged (13000×g, 10 min, 20 °C), the supernatant was discarded, and the washed sludge was again extracted with 70% ethanol for 30 min at 40 °C. This operation was repeated until no more sugar was detected in the liquid phase with the sulphuric phenol method (Dubois, Gilles, Hamilton, Rebers, & Smith, 1956). The numbers of consecutive extractions needed to eliminate all sugars were in total 5 for skins, 6 for fresh flesh, and 11 for withered flesh. Then, AISs were further washed twice with 96% ethanol and once with acetone. After drying under air flux overnight to evaporate the acetone, the purified AISs powders obtained were used for the analysis of polysaccharides composition.

2.8. Polysaccharide composition of AISs determined by gas chromatography methods

The carbohydrate composition of the skins and flesh AISs was estimated by three gas chromatography (GC) methods using a Shimadzu GCMS-QP2010SE gas chromatograph equipped with a split/splitless inlet and a flame ionization detector (FID, Shimadzu, Kyoto, Japan). The DB225 capillary column (30 m × 0.25 mm i.d., 0.25 µm film) or DB-1 capillary column (30 m × 0.25 mm i.d., 0.25 µm film) was used for the analytical separation and hydrogen 5.6 B50 was the carrier gas.

To study the molar percentage composition of neutral and acidic glycosyl-residue of AISs polysaccharides, the per-*O*-trimethylsilylated methyl glucoside derivatives (TMS) method was applied. Methanolysis for 16 h at 80 °C and trimethylsilylation were performed following the method detailed by Doco, O'neill, and Pellerin (2001).

To determine the neutral glycosyl-residue content of pectic and hemicellulose polysaccharides, the conversion of neutral sugars into volatile alditol acetate derivatives was performed after polysaccharide hydrolysis with trifluoroacetic acid (TFA, 120 °C, 75 min), as described by Apolinar-Valiente et al. (2015). One hundred microliters of 1 mg/mL inositol and allose solutions were used as internal standards. In combination with the alditol acetates procedure, a further hydrolysis with 72% sulphuric acid was applied to quantify the cellulose present in AISs carbohydrates, according to the method proposed by Hoebler, Barry, David, and Delort-Laval (1989) based on the first studies of Seaman, Moore, Mitchell, Millett (1954). All the analyses have been performed in triplicate.

2.9. Comprehensive Microarray Polymer Profiling analyses (CoMPP)

For the purification phase, 10 g of flesh frozen powder or 2 g of skins frozen powder were mixed with 30 mL of absolute ethanol and immediately transferred to 80 °C water-bath for 15 min to inactivate the enzymes. After cooling to room temperature, each of the three replicates for every sample were centrifuged (1030 g, 4 °C, 10 min) in a Hettich 4–16 KS centrifuge (Tuttlingen, Germany) and the supernatant was discarded. The remaining pellet was subjected to a series of solvent washes using methanol, chloroform, and acetone according to the method described by Gao, Fangel, Willats, Vivier, and Moore (2015). The liquid-to-solid ratio was 3:1 (v/v) for each of the six washing-step. Then, the pellet was dried for 20 min in the fume hood and re-suspended in ice-cold ultrapure water and freeze-dried to generate the alcohol insoluble residue (AIR) to retain the soluble polymers for the Comprehensive Microarray Polymer Profiling analysis (CoMPP). Once freeze-dried, 10.00 mg of AIR for each replicate were precisely weighted in 1.2 mL polypropylene Collection Microtubes (QIAGEN, Hilden, Germany) and extracted in 300 µL of cyclohexane-diamino-tetraacetic acid (CDTA, 50 mM, pH 7.5). Each biological replicate was used to generate 6 replicates. A glass bead was added to each tube and the extraction solution have been homogenized at a frequency of 30 Hz for 2 min and then 6 Hz for 2 h. The soluble pectin-rich fraction (CDTA-fraction) obtained were collected after centrifugation by taking the supernatant. The remaining pellet was re-extracted using 300 µL of NaOH (4 M + 0.1% NaBH₄) following the same agitation procedure, obtaining a hemicellulose-rich fraction (NaOH-fraction). Pectin and hemicellulose-rich fractions (CDTA-fraction and NaOH-fraction respectively) were pipetted into 384-microwell plates and printed into nitrocellulose membrane (0.45 mm pore size, Whatman, Maidstone, UK) using a microarray robot (Sprint, Arrayjet, Roslin, UK). The printed arrays were incubated with several monoclonal Antibodies (mAbs) and Carbohydrate Binding Modules (CBMs) listed in Table S1. The arrays were scanned at 2400 dots/inch with a CanoScan 880F, Soborg, Denmark). The software Array-Pro Analyzer 6.3 was used to quantify probe signals (Media Cybernetics, Rockville, Maryland, USA), as described by Gao, Fangel, Willats, Vivier, and Moore (2021). The raw data were normalized and converted into a heatmap for visualization. The relative abundances of different polymers epitopes are displayed on a scale of 0–100. The values are means from three biological repeats and four dilutions.

2.10. Statistical analysis

Statistical analysis was carried out using R statistic software version 3.6.2 (R Foundation for Statistical Computing, Vienna, Austria). The homoscedasticity and normality of the data were tested by using Levene's and Shapiro Wilk's tests. One-way analysis of variance (ANOVA) using the Tukey HSD post-hoc test was used to evaluate significant differences among treatments. Differences were considered statistically significant at p -value <0.05. T-test was used to discriminate significant differences between the two different withering conditions. Pearson's correlation coefficients were calculated to determine significant relationship between seeds phenolic composition and extraction yields, and tannin composition quantified by HPSEC and spectrophotometric analyses. Principal component analysis (PCA) was performed on the raw data set of CoMPP results of the AISs skins and flesh cell walls to better understand the differences among treatments.

3. Results and discussion

Fig. 1 shows the environmental conditions recorded during the withering period under sun uncontrolled withering (SUN, a) and controlled withering in the "fruttaio" dehydration room (CTR, b). The graphs reported the daily minimum, maximum, and average values of temperature (°C) and relative humidity (%). The grapes withered

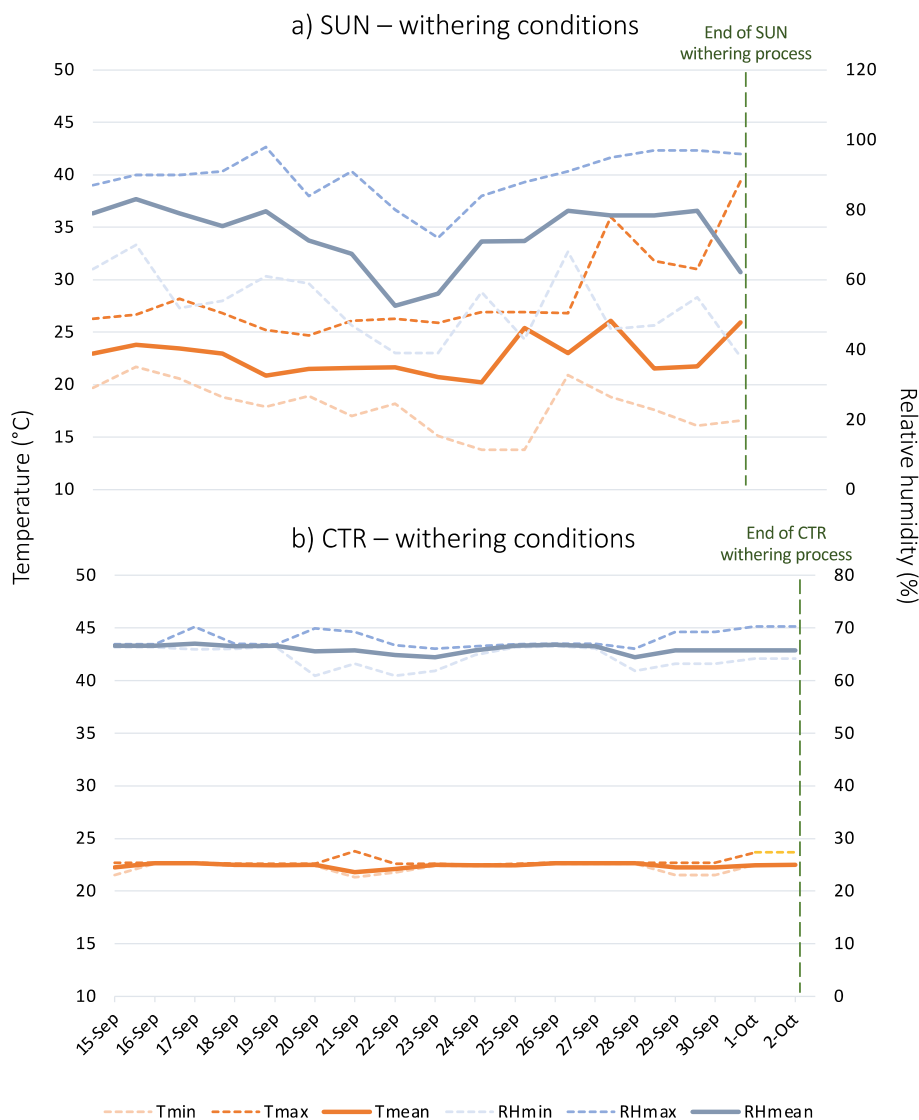


Fig. 1. – Thermohygrometric conditions of uncontrolled-sun (SUN, a) and controlled-*fruttai* (CTR, b) withering. Tmin: minimum daily temperature; Tmax: maximum daily temperature; Tmean: average daily temperature; RHmin: minimum daily relative humidity, RHmax: maximum daily relative humidity; RHmean: average daily relative humidity values.

outside under the sun were subjected to very variable conditions ranging between 14 and 40 °C of temperature (although only for short periods up to 35 °C) and 38–98 % relative humidity. For SUN the withering lasted 15 days in total until reaching the 30% WL goal. Instead, the controlled environmental conditions of CTR had a lower range of variation (22 ± 1 °C temperature range and 61–70% relative humidity) and grapes reached 30% WL in 17 days.

3.1. Grape must composition and berry texture analysis

Grape must technological parameters and berry mechanical properties determined before the withering (FRESH) and after the dehydration process in the two modalities (SUN and CTR) are shown in Table 1. As expected, significantly higher total soluble solids (°Brix) contents were found in withered grapes with respect to the fresh sample ($p < 0.01$), increasing from 24.7 to 37.4–38.9 °Brix. Considering that the same weight loss of 30% was achieved for both processes, different dehydration techniques did not determine statistically significant differences between them (p -value of the T-test SUN vs CTR = 0.253).

The pH value was significantly higher in SUN samples than CTR

ones. This value increased significantly in SUN-dehydrated grapes (+0.32 and +0.25 units compared to FRESH and CTR grapes, respectively), whereas CTR experienced a slight increase in pH values (+0.07) that was not significant compared to FRESH sample. The increase in pH values during withering has already been observed in previous studies (Bellincontro et al., 2016) on Corvina, Corvinone, and Rondinella, and it is probably due to a greater release of cations (mainly K^+) from the cell's vacuoles of flesh and skins to compensate water loss maintaining the pressure of cellular turgor (Zoccatelli et al., 2013). Indeed, berry pH is a function of the levels of organic acids and cations (Boulton, 1980) and the thermohygrometric features (i.e. higher temperature, sun exposure, different relative humidity values) affect indirectly the pH via the levels of acids and cations uptake during dehydration (Barnaud, Zerihun, Gibberd, & Bates, 2014). Several authors attribute the greater effect on pH values modifications to elevated temperature rather than light exposure (Bergqvist, Dokoozlian, & Ebisuda, 2001; Martínez De Toda & Balda, 2014). Thus, possibly, higher temperature stress may explain the reason for the differences between the two withering modes studied.

Titrate acidity was also affected differently by the two withering modalities (T-test p -value < 0.01): in CTR grapes it was preserved and

Table 1

– Standard chemical parameters and mechanical properties of Aleatico grapes at harvest (FRESH) and after withering at 30% WL under sun natural withering (SUN) and controlled conditions in *fruttaio* (CTR).

Parameter	<i>fresh grapes</i>	<i>withered grapes 30 % WL</i>		Sign. ^a ANOVA	Sign. ^b T- test
	FRESH	SUN	CTR		
Grape must technological parameters					
Total soluble solids (°Brix)	24.7 ± 0.4 b	38.9 ± 1.5 a	37.4 ± 1.2 a	***	ns
pH	3.31 ± 0.02 b	3.63 ± 0.04 a	3.38 ± 0.05 b	***	**
Titrateable acidity (g/L tartaric acid)	5.79 ± 0.11 b	5.08 ± 0.13 c	6.14 ± 0.06 a	***	**
Mechanical properties					
F _{sk} (N)	0.63 ± 0.12	0.73 ± 0.20	0.64 ± 0.17	ns	ns
W _{sk} (mJ)	0.66 ± 0.22 b	1.01 ± 0.40 a	0.97 ± 0.41 a	***	ns
E _{sk} (N/mm)	0.27 ± 0.05 a	0.20 ± 0.04 b	0.16 ± 0.03 c	***	**
Sp _{sk} (µm)	232 ± 47 b	304 ± 56 a	290 ± 55 a	***	ns
F _{ped} (N)	2.24 ± 0.57 a	1.36 ± 0.50 b	1.29 ± 0.47 b	***	ns
W _{ped} (mJ)	1.31 ± 0.60	1.38 ± 0.58	1.44 ± 0.85	ns	ns

All data are expressed as average value ± standard deviation (n = 3 and n = 40 for Grape must technological parameters and Mechanical properties, respectively). Sign: ***, **, and ns indicate significance at p < 0.001, 0.01, and not significant differences, respectively, among treatments (FESH, SUN and CTR) and between the two withering modalities (SUN, CTR) according to ANOVA^(a) and T-tests^(b). Different Latin letters among the same raw indicate significant differences^(a) according to Tukey-b test (p < 0.05) for ANOVA. F_{sk}: berry skin maximum break force; W_{sk}: berry skin break energy; E_{sk}: skin resistance against deformation; Sp_{sk}: berry skin thickness; F_{ped}: peduncle detachment force; W_{ped}: energy needed for peduncle detachment.

increased (from 5.79 of the FRESH to 6.14 g/L of the CTR, expressed as tartaric acid), while SUN samples experienced a loss in titrateable acidity with respect to the FRESH (from 5.79 of FRESH to 5.08 g/L as tartaric acid of SUN grapes). In fact, as demonstrated in other studies, titrateable acidity may increase or decrease depending on the dehydration temperature in function of the balance concentration/degradations of grapes organic acids (Chkaiban et al., 2007; Constantinou, Gómez-Caravaca, Goulas, Segura-Carretero, & Manganaris, 2017).

Regarding mechanical properties, no significant differences among samples were found for the maximum skin break force values (F_{sk}), whereas the break energy (W_{sk}) was significantly higher for withered grapes with respect to the fresh ($\Delta W_{sk} = 0.35\text{--}0.31$ mJ). However, no significant differences between the two dehydration modalities were found (T-test p-value = 0.725), probably due to the high variability among the dehydrated berries. Similarly, Sp_{sk} showed increased values in withered grapes with respect to the fresh material (+31% and +25% for SUN and CTR, respectively) coherently with the previous observations on Mondeuse, Nebbiolo and Barbera on-vine and off-vine dehydrated grapes (Rolle et al., 2009; <link id=bib_río_segade_et_al_2019a>Río Segade, Pissoni, Giacosa, et al., 2019; </link>). However, no significant differences were found between SUN and CTR at the same WL% (T-test p-value = 0.356). FRESH Aleatico berries featured skin hardness (assessed by F_{sk} and W_{sk} parameters) and thickness (Sp_{sk}) values very similar to cv. Moscato white grapes (Giacosa et al., 2019), of which Aleatico is genetically descendant (D'Onofrio et al., 2021).

The skin resistance to the axial deformation during the puncture test (E_{sk}), instead, experienced significant differences among the withering modalities studied. Indeed, Aleatico E_{sk} decreased significantly after

dehydration for both the methods, particularly for CTR (−27% and −41% from fresh to SUN and CTR, respectively). Therefore, the withering increased skin elasticity in Aleatico berries. Interestingly, grape skins withered under controlled conditions were significantly less rigid than sun-dehydrated samples (T-test p-value < 0.01). These differences could be due to the reorganization of skin cells and to the modifications of cell wall polysaccharides. Indeed, Fasoli et al. (2019), studying the morphological alterations in skin sections of cv. Corvina during withering, evidenced a gradual cell disorganization from fresh to different postharvest withering phases that could explain the differences shown between fresh and withered samples.

The peduncle detachment force (F_{ped}) obtained by traction (tension) test decreased markedly after grape dehydration in both modalities (−39% and −42% for SUN and CTR, respectively), with no significant differences between SUN and CTR samples (T-test p-value = 0.533). The average values measured at 30% WL for both SUN (1.36 N) and CTR (1.29 N) treatments suggested that, regardless of the withering modality, Aleatico berries had a great propensity to fall throughout the process if subjected to vertical bunch placement such as hanged clusters system or on-vine postharvest ripening (Rolle et al., 2009). Thus, it would be more suitable to place Aleatico grapes in horizontal bunch post-harvest withering systems such as single-layer plastic boxes or reed mats, independently of the withering conditions chosen.

3.2. Potential and extractable phenolic profiles

With the aim of showing the changes in the extractable phenolic composition in wine-like conditions (EXT) during maceration from an oenological applicative point of view, considering the loss of juice inside the dehydrated berries, the data of Fig. 2 (a, c) were expressed in mg/kg of berries to better represent the practical situation under winemaking and provide tools in the choice of the maceration strategy for withered grapes. However, the final content of phenolic compounds in withered grapes is the result of a balance between concentration and metabolic losses of compounds occurring within the berry during the withering process (De Rosso et al., 2016). For this reason, the data of the detailed potential (POT) and extractable (EXT) phenolic profiles at the end of the simulated maceration were expressed, in Table 2, per grape-portions weight (mg/g of skins, seeds, or flesh), to avoid the influence of the whole berry weight loss and consider the chemical modifications occurring within the different berry's portions due to metabolism separately from the concentration effect.

Skin anthocyanins are the clearest example of the modifications described above. In fact, as regards potential TAntI in grapes expressed as mg/g skins (Table 2), sun-dehydrated grapes showed the lowest content, which was statistically different with respect to FRESH and CTR (ANOVA p-value < 0.01; T-test SUN vs CTR p-value = 0.049). TAntI (mg/g skins) decreased after withering also in CTR sample, but to a lesser extent than in SUN one. There was then no statistically difference between CTR and FRESH grapes. In fact, as demonstrated by Mencarelli et al. (2010), the withering temperature plays a central role in the losses of anthocyanins after dehydration, which are probably more strongly degraded at higher temperatures due to the oxidative activity of enzymes such as polyphenol oxidase (PPO) or peroxidase, and maybe also to a decrease of their possible synthesis as the gene expression of phenylalanine ammonia lyase (PAL) was downregulated. Moreover, the exposition to direct sunlight of the bunches withered in SUN mode may have contributed to the decrease of anthocyanins compounds, as previously observed by several authors (Spayd, Tarara, Mee, & Ferguson, 2002; Sternad Lemut, Sivilotti, Franceschi, Wehrens, & Vrhovsek, 2013). Indeed, although sunlight exposure play an important role in stimulating the anthocyanin biosynthesis, the stress caused by excessive photosynthetically active radiation (PAR) and UV radiation can activate antioxidant defence mechanisms, causing anthocyanins degradation (Gambetta, Holzapfel, Stoll, & Friedel, 2021). Interestingly, when expressed in mg/kg of berries (Table S2), potential TAntI content tended

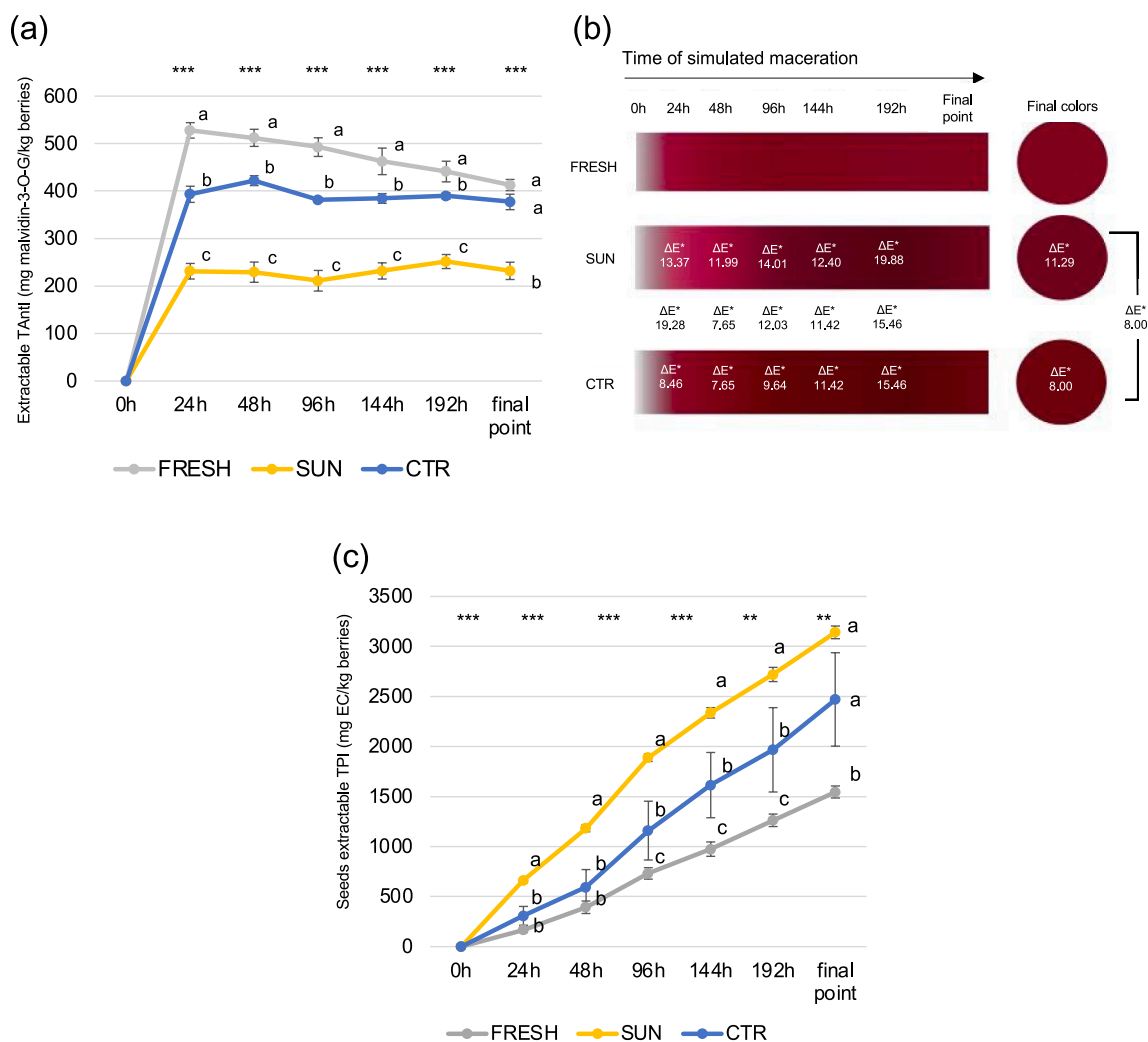


Fig. 2. – Evolution of different parameters during the simulated macerations in wine-like solutions of skins and seeds. a: skin extractable anthocyanins (TAntI); b: visual color of the skin wine-like extracts (CIEL*a*b* coordinates converted to RGB 24-bit color values); c: seed extractable polyphenols (TPI). Malvidin-3-O-G: malvidin-3-O-glucoside; EC: (–)-epicatechin. All data are expressed as average value \pm standard deviation ($n = 3$). Sign: *** and ** indicate significance at $p < 0.001$, and 0.01 , respectively, for the differences among fresh material before the withering (FRESH), sun-withered grapes (SUN) and withered grapes in controlled conditions (CTR) at each maceration time. Latin letters for each sampling point indicate significant differences according to Tukey-b test ($p < 0.05$) for ANOVA. ΔE^* values between FRESH and withered grapes (SUN or CTR) during macerations are reported in white inside the colored bars at the correspondent points, while ΔE^* values between SUN and CTR are reported in black between the correspondent bars; ΔE^* values among treatments at the end of the process are shown inside the circle corresponding to the final visual color.

to slightly increase by an average of +108 mg/kg for CTR (average withering temperature of 22.5 °C) and to decrease for SUN (average withering temperature of 27 °C) by –67 mg/kg with respect to the FRESH. This suggests that the concentration effect compensated for the slight losses of TAntI (mg/g skins) in CTR, but it was not enough to offset the greater loss of anthocyanins in SUN.

The anthocyanin profiles (Table 2) confirmed that a greater oxidation occurred within the skins of sun-exposed grapes for all the anthocyanin forms. It is important to consider that only a part of these compounds is extracted in wine-like conditions (Abi-Habib et al., 2021), reason why the study of both the potential and extractable components provides very useful information. Indeed, anthocyanins extraction yields (%) were quite different among the three conditions studied: the final TAntI extraction yield in wine-like solution for FRESH (72%) was higher than CTR one (55%), which was itself higher than SUN one (46%). These differences in extractability combined with the degradation observed in potential TAntI after berry dehydration, resulted in a lower content of extractable anthocyanins in withered grapes with a greater extent for

sun-dehydrated grapes (p-value of the T-test SUN vs CTR < 0.001). Moreover, anthocyanins were slightly more extracted than acetylated ones, which were much more extracted than the cinnamoylated forms at the end of the simulated macerations (Table 2), in accordance with previous findings (Abi-Habib et al., 2021). The extraction depended both on the structure of the anthocyanin and on the withering modality. Indeed, the extraction yields of the different anthocyanin forms followed the same trend of TAntI (FRESH > CTR > SUN). The lower extractions of anthocyanins and flavanols observed in sun-dehydrated grapes represent a disadvantage also for the long-term color stability, since the formation of polymeric pigments is very important to this purpose (Cheynier et al., 2006).

A pattern similar to TAntI was observed for POT phenolic content from skins (total phenolics-TPI and condensed tannins-CT), although the tannin amount was not significantly affected by the different withering methods when expressed in mg/g skins (Table 2). In line with anthocyanins, the skin extraction yields (%) decreased significantly from fresh to withered grapes, with a greater extent in SUN also for TPI and CT

Table 2

– Potential and extractable phenolic composition at the end of the simulated maceration in a wine-like solution of fresh (FRESH), and withered Aleatico grapes under the sun (SUN) or in *fruttai*-controlled conditions (CTR).

Compound	Potential/Extractable	<i>fresh grapes</i>			<i>withered grapes</i>		Sign. ^a ANOVA	Sign. ^b T-test
		FRESH	SUN	CTR	SUN	CTR		
Skins								
TPI (mg EC/g skins)	Potential	41 ± 3 a	30 ± 3 b	35 ± 3 ab	*	*		
	Extractable	27 ± 3 a	11 ± 0 c	18 ± 1 b	***	***		
	Extraction yield (%) [#]	60 ± 5 a	40 ± 6 c	49 ± 1 b	***	***		
TANtI (mg Mv-3-G/g skins)	Potential	6 ± 1 a	4 ± 0 b	5 ± 1 ab	**	*		
	Extractable	5 ± 0 a	2 ± 0 c	3 ± 0 b	***	***		
	Extraction yield (%) [#]	72 ± 8 a	46 ± 9 b	55 ± 4 b	***	*		
CT (mg EC/g skins)	Potential	17 ± 2	14 ± 1	14 ± 1	ns	ns		
	Extractable	8 ± 0 a	3 ± 0 c	5 ± 0 b	***	***		
	Extraction yield (%) [#]	41 ± 4 a	29 ± 4 b	33 ± 1 b	***	ns		
FRV (mg C/g skins)	Potential	7 ± 0 a	3 ± 0 c	5 ± 1 b	***	*		
	Extractable	5 ± 0 a	2 ± 0 c	3 ± 0 b	***	***		
	Extraction yield (%) [#]	57 ± 3	58 ± 7	60 ± 14	ns	ns		
FRV/CT	Potential	0.42 ± 0.06 a	0.21 ± 0.02 b	0.32 ± 0.08 ab	*	ns		
	Extractable	0.58 ± 0.02 a	0.43 ± 0.02 b	0.58 ± 0.01 a	***	***		
Anthocyanin profile (mg Mv-3-G/g skins)								
Dp-3-G	Potential	0.25 ± 0.04 a	0.08 ± 0.01 b	0.13 ± 0.02 b	**	*		
	Cy-3-G	0.04 ± 0.01 a	0.02 ± 0.00 b	0.02 ± 0.00 b	*	ns		
	Pt-3-G	0.28 ± 0.04 a	0.11 ± 0.02 b	0.16 ± 0.03 b	**	ns		
Pn-3-G	Potential	0.26 ± 0.05 a	0.13 ± 0.02 b	0.13 ± 0.03 b	*	ns		
	Mv-3-G	2.95 ± 0.52 a	1.40 ± 0.19 b	1.97 ± 0.31 b	**	ns		
	∑ Acetyl-G	0.62 ± 0.11 a	0.23 ± 0.03 b	0.33 ± 0.07 b	**	ns		
∑ Cinnamoyl-G	Potential	1.21 ± 0.97 a	0.60 ± 0.10 b	0.91 ± 0.13 ab	**	*		
	Dp-3-G	0.08 ± 0.02 a	0.01 ± 0.00 b	0.02 ± 0.00 b	***	ns		
	Cy-3-G	0.02 ± 0.01 a	0.00 ± 0.00 c	0.01 ± 0.00 b	***	**		
Pt-3-G	Potential	0.13 ± 0.02 a	0.03 ± 0.00 c	0.05 ± 0.00 b	***	**		
	Pn-3-G	0.16 ± 0.02 a	0.03 ± 0.01 b	0.05 ± 0.01 b	***	*		
	Mv-3-G	2.16 ± 0.23 a	0.58 ± 0.04 c	1.06 ± 0.13 b	***	**		
∑ Acetyl-G	Potential	0.38 ± 0.04 a	0.08 ± 0.00 c	0.16 ± 0.02 b	***	**		
	∑ Cinnamoyl-G	0.42 ± 0.08 a	0.11 ± 0.06 b	0.24 ± 0.03 b	***	**		
	∑ -G	69 ± 12 a	35 ± 9 c	50 ± 9 b	***	**		
∑ Acetyl-G	Extraction yield (%)	61 ± 12 a	35 ± 4 c	48 ± 12 b	***	**		
	∑ Cinnamoyl-G	35 ± 8 a	18 ± 4 c	26 ± 5 b	***	**		
	Extraction yield (%)							
Phenolic acids (mg/g skins)								
Caftaric acid	Potential	0.19 ± 0.01 a	0.05 ± 0.02 c	0.09 ± 0.01 b	***	*		
	Extractable	0.10 ± 0.01 a	0.01 ± 0.00 b	0.02 ± 0.00 b	***	*		
	Extraction yield (%) [#]	30 ± 3 a	9 ± 4 c	16 ± 2 b	***	***		
Coutaric acid	Potential	2.09 ± 0.15 a	0.31 ± 0.13 b	0.65 ± 0.19 b	***	ns		
	Extractable	0.76 ± 0.20 a	0.04 ± 0.01 b	0.06 ± 0.02 b	***	ns		
	Extraction yield (%) [#]	21 ± 4 1 a	12 ± 6 b	6 ± 2 c	***	*		
Flesh								
Phenolic acids (mg/g flesh)								
Caftaric acid	Potential	0.10 ± 0.01 ab	0.07 ± 0.02 b	0.11 ± 0.01 a	*	*		
Coutaric acid	Potential	0.05 ± 0.01	0.03 ± 0.01	0.04 ± 0.01	ns	ns		
Seeds								
TPI (mg EC/g seeds)	Potential	149 ± 8	149 ± 4	155 ± 2	ns	ns		
	Extractable	54 ± 5 b	77 ± 2 a	57 ± 9 b	**	*		
	Extraction yield (%) [#]	30 ± 3 b	41 ± 6 a	34 ± 6 b	*	*		
CT (mg EC/g seeds)	Potential	90 ± 6	89 ± 9	85 ± 2	ns	ns		
	Extractable	22 ± 9	41 ± 12	22 ± 7	ns	ns		
	Extraction yield (%) [#]	21 ± 7 b	38 ± 11 a	25 ± 7 ab	***	**		
FRV (mg C/g seeds)	Potential	94 ± 10	85 ± 6	89 ± 6	ns	ns		
	Extractable	31 ± 5 b	46 ± 2 a	33 ± 6 b	*	*		
	Extraction yield (%) [#]	28 ± 4 c	45 ± 2 a	34 ± 7 b	***	***		
FRV/CT	Potential	1.04 ± 0.10	0.95 ± 0.04	1.05 ± 0.09	ns	ns		
	Extractable	1.58 ± 0.75	1.20 ± 0.33	1.50 ± 0.59	ns	ns		

All data are expressed as average value ± standard deviation (n = 3). Sign: ***, **, * and ns indicate significance at p < 0.001, 0.01, 0.05 and not significant differences, respectively, among treatments (FRESH, SUN and CTR) and between the two different withering modalities (SUN, CTR) according to ANOVA^(a) and T-tests^(b). Different Latin letters among the same raw indicate significant differences^(a) according to Tukey-b test (p < 0.05) for ANOVA. TPI: total phenolic index; TAN: total anthocyanins; CT: condensed tannins by methyl cellulose assay; FRV: flavanols reactive to vanillin; Dp-3-G: delphinidin-3-glucoside; Cy-3-G: cyanidin-3-Glucoside; Pt-3-G: petunidin-3-glucoside; Pn-3-G: peonidin-3-glucoside; Mv-3-G: malvidin-3-glucoside; -G: simple glucosides; Acetyl-G: acetylated glucosides; Cinnamoyl-G: cinnamoylated glucosides; EC: epicatechin; C: catechin; #: extraction yields (%) are calculated using the data expressed as mg/kg berries.

(TPI: 20 and –11%; CT: 12 and –8% for SUN and CTR with respect to FRESH, respectively).

Instead, as regards POT monomeric and low-molecular weight flavanols (FRV), a strong decrease for both withering methods with respect to FRESH was observed considering both data expressed in mg/g skins (ANOVA p-value < 0.001, Table 2). The loss of FRV detected in withered

skins was higher for SUN, possibly due to polymerization phenomena light induced, as the result of the penetration of H₂O₂ into vacuoles of epidermal cells (Gambetta et al., 2021). Moreover, the extraction yields of FRV were not significantly different among FRESH, SUN, and CTR skins (57–60%). Indeed, although flavan-3-ols and low-molecular tannins can access more sites, their interactions with skin cell walls are

thought to be negligible, explaining that they are more easily desorbed (Bindon et al., 2014) and not affected by the skin cell wall polysaccharide modifications observed among treatments, unlike other phenolic compounds. Consequently, the FRV/CT ratio of SUN skins was lower than those of FRESH and CTR, indicating a potential softening effect in the mouth-feel perception of the wine due to the lower proportion of low-molecular weight tannins, which are held responsible for bitterness and “green taste” astringency sensations (Busse-Valverde, Gomez-Plaza, Lopez-Roca, Gil-Munoz, & Bautista-Ortin, 2011).

Therefore, at the end of the 10-days simulated maceration of skins in wine-like solutions, the EXT profile of the sun-dehydrated grape skins showed the lowest contents of polyphenols, anthocyanins, phenolic acids, and tannins, but also a lower percentage of low-polymerized forms on the total condensed tannins (when expressed both as mg/kg of berries and mg/g of skins). Instead, the EXT phenolic profile of CTR was not significantly different from the profile of FRESH grape skins when expressed as mg/kg of berries, excepting for phenolic acids whose contents decreased significantly for CTR samples (Table S2).

The POT contents of hydroxycinnamic acid (HCAs) esters detected in skins and flesh (mg/g skins or flesh, Table 2) confirmed the greater loss of compounds of sun-dehydrated Aleatico grapes, whereas in controlled conditions these compounds were better preserved, as reported by Frangipane et al. (2012). Indeed, the oxidation of coumaric and caftaric acids by PPO plays a crucial role in the coupled oxidation phenomena of the other phenolic compounds (Cheynier, Basire, & Rigaud, 1989). The lower amounts of skin HCA esters found in wine-like extracts of withered grapes, particularly for SUN, were possibly due to the implication of these compounds in other reactions during the maceration, as supposed by Marquez, Serratos, Lopez-Toledano, and Merida (2012). However, the ratio (%) of cinnamoylated forms in the anthocyanin profiles resulted not significantly affected by the treatment (Table S2), suggesting a more probable involvement of HCAs in oxidation rather than in the formation of *p*-coumaroylated anthocyanins. The higher proportion of yellow color component (A₄₂₀) with respect to the red component (A₅₂₀) found in SUN grapes (hue, Table S3) could be related to the browning of the extracts due to oxidation, or to the formation of anthocyanin-derived pigments such as pinotins (Scalzini, Giacosa, Rio Segade, Paissoni, & Rolle, 2021).

Regarding seeds, no significant differences were found among FRESH, SUN and CTR samples for the phenolic parameters (TPI, CT, FRV) expressed in mg/g seeds (Table 2), indicating that oxidation did not occur, or that oxidation was balanced to a possible synthesis of seed polyphenols during dehydration, as supposed by Centioni, Tiberi, Pietromarchi, Bellincontro, and Mencarelli (2014) for cv. Cesanese grape seeds. Moreover, an increased potential content as expressed in mg/kg berries basis could be due to a concentration effect attributable to the juice loss in the whole berry after dehydration (SUN and CTR, Table S2), as it was demonstrated that during withering the seed weight remains almost constant until reaching 60% WL (Rio Segade et al., 2016).

Concerning the contents of EXT phenolics in seeds, in wine-like conditions TPI, CT, and FRV increased both on mg/g and mg/kg basis from fresh to withered grapes (Table 2, Table S2), following the same trend described for TPI during the maceration process (mg/kg of berries): SUN > CTR > FRESH (Fig. 2c). Some other authors demonstrated an increase of extractable proanthocyanidins and oligomeric flavanols in the seeds of dehydrated grapes compared with fresh grapes, in accordance with these findings (Moreno et al., 2008; Rolle et al., 2013).

Opposite to what was observed for skins, the extractability of phenolic compounds in seeds increased after withering, particularly for SUN whose percentage yields were higher than for FRESH and CTR samples for all the parameters studied. Also, the extractability for CTR increased compared with FRESH, but the yield was weaker than for SUN (+4, +4, and +6% for TPI, CT and FRV, respectively). FRV/CT ratio was always lower for SUN samples as observed for skins, although in seeds the differences were not statistically significant.

The increased extraction yields for withered grape seeds are in accordance with the few studies present in the literature concerning the effect of grape dehydration on the extractability of phenolic compounds from seeds (Centioni et al., 2014; Río Segade et al., 2016). Moreover, for the first time, the greater extractability of polyphenols, proanthocyanidins and low-molecular weight flavanols in grape seeds of sun-dehydrated grapes vs in-room dehydration was shown. Rolle et al. (2009) highlighted a decreasing tendency of seed hardness after the on-vine dehydration process, opposite to the hardening of the seeds occurring throughout the ripening. The softening of seed tissues induced by dehydration could explain the modifications observed in withered grapes compared to fresh grapes. It may be hypothesized that high temperatures, to which the sun-dehydrated grapes were subjected, intensified the softening of seeds, leading to higher extraction yields in SUN compared to CTR. However, as there are no studies on the anatomical and histological changes in seeds during grape dehydration, and due to the presence of the secondary cell walls in seeds (Hanlin et al., 2010), more precise hypotheses require further targeted studies. In particular, the secondary cell walls in seeds, which contain lignin and more cellulose than skins, may justify the differences observed among treatments in the extractability of FRV from seeds that were not evidenced on skins.

3.3. Extraction kinetics and color implications

As previously mentioned, Fig. 2 shows the gradual extraction of anthocyanin compounds from Aleatico FRESH, SUN and CTR skins (a), the parallel evolution of the visual color (b), and the extraction of total polyphenols (TPI) from the seeds (c) during the macerations in wine-like solutions.

The anthocyanin contents found during the simulated fermentative maceration are in line with the values detected in real winemaking conditions (Cotarella, 2013). Throughout the simulated process, the progressive solubilisation of anthocyanins showed significant differences among the samples studied (Fig. 2a). The anthocyanins diffusion in wine-like solutions was higher and faster in fresh grapes with respect to the withered ones. For FRESH grapes, the data showed a rapid rise of TAntI content, which reached a maximum at 24h (523 mg/kg of berries), followed by a normal decreasing trend of these compounds to 413 mg/kg of berries after 10 days of maceration. This trend was probably due to oxidation, polymerization reactions and readsorption on the skins, and confirms the importance of the early maceration steps in the color traits of the final wine (Paissoni et al., 2020) also for Aleatico grapes, although it is a variety rich in stable forms (above 50% of malvidin-3-*O*-glucoside and >20% acylated glucosides; Mattivi, Guzzon, Vrhovsek, Stefanini, & Velasco, 2006). Nevertheless, at the end of the process, FRESH samples still had the highest content of extractable TAN in wine-like conditions (+43% and +8% than SUN and CTR final TAntI contents, respectively). For withered samples, instead, the TAntI diffusions from the skin were slower, especially for SUN samples with a maximum content reached after 24–48 h. This delay is probably related to the higher Sp_{sk} of withered grape skins, as previously postulated (Rolle, Torchio, Zeppa, & Gerbi, 2008; Río Segade, Giacosa, Gerbi, & Rolle, 2011; Río Segade, Orriols, Giacosa, & Rolle, 2011), as well as the modifications in cell wall composition. However, the red pigment content after 48h of skin simulated extraction remained more stable in withered samples than in FRESH ones, probably because the delay in extraction allowed to better preserve the more easily extractable and degradable anthocyanin forms (i.e. cyanidin-3-*O*-glucoside and peonidin-3-*O*-glucoside; González-Neves, Gil, & Barreiro, 2008). Indeed, although the kinetics of the two different withering methods were similar, CTR grapes had on average + 41% higher amounts of extractable anthocyanins than SUN throughout the entire process.

The differences detected in the content of extractable anthocyanins in wine-like conditions influenced the color of extracts during the simulated macerations. Fig. 2b shows the visual colors obtained by the

conversion of the CIELab coordinates (Table S3) in the corresponding color on RGB scale, which is comparable to the shades perceived by the human biological visual system Cheng, Jiang, Sun, & Wang, 2001; Río Segade, Paissoni, Vilanova, et al., 2019; Scalzini et al., 2020). The progressive solubilisation of anthocyanins reflects color features of the macerating extracts particularly for SUN samples, which experienced a major color change after 96 h of maceration. However, the different shades perceived progressively during the SUN samples wine-like maceration seemed to be related only to the color intensity and not to the hue, which did not show significant differences among the six SUN sampling points. Indeed, from the beginning of the simulated process, SUN extracts showed significantly higher values of hue with respect to the others extracts, reaching at the final point +0.148 and +0.092 hue units versus FRESH and CTR, respectively, meaning a major yellow color component (A_{420}) with respect to the red one (A_{520}). At the end of the maceration (240 h), the extracts color of the three samples showed differences perceptible by the human eye (Martínez, Melgosa, Pérez,

Hita, & Negueruela, 2001, Fig. 2b), with a colorimetric difference (ΔE^*) of 11.29 and 8.00 respectively for SUN and CTR in relation to FRESH, and a ΔE^* of 8.00 between CTR and SUN samples.

As regards seed extraction kinetics (Fig. 2c), the amounts of EXT polyphenols (TPI, mg/kg of berries expressed as (-)-epicatechin) increased progressively with the increasing maceration time for the three samples studied. In accordance with the literature, the higher is the ethanol concentration, the greater is the diffusion of polyphenols from seeds (Canals, Llaudy, Valls, Canals, & Zamora, 2005). Under the same ethanol concentration, this trend was more remarkable for seeds of withered grapes, particularly for sun-dehydrated samples. Indeed, for the whole maceration time, the TPI of SUN grapes resulted higher than CTR (with an average of +65%), and that of CTR was higher than FRESH (on average +62%). However, even if throughout the maceration the differences in TPI between the two dehydration modalities studied were statistically significant at each sampling point until 192 h, at the end of the maceration no significant differences were found in polyphenols

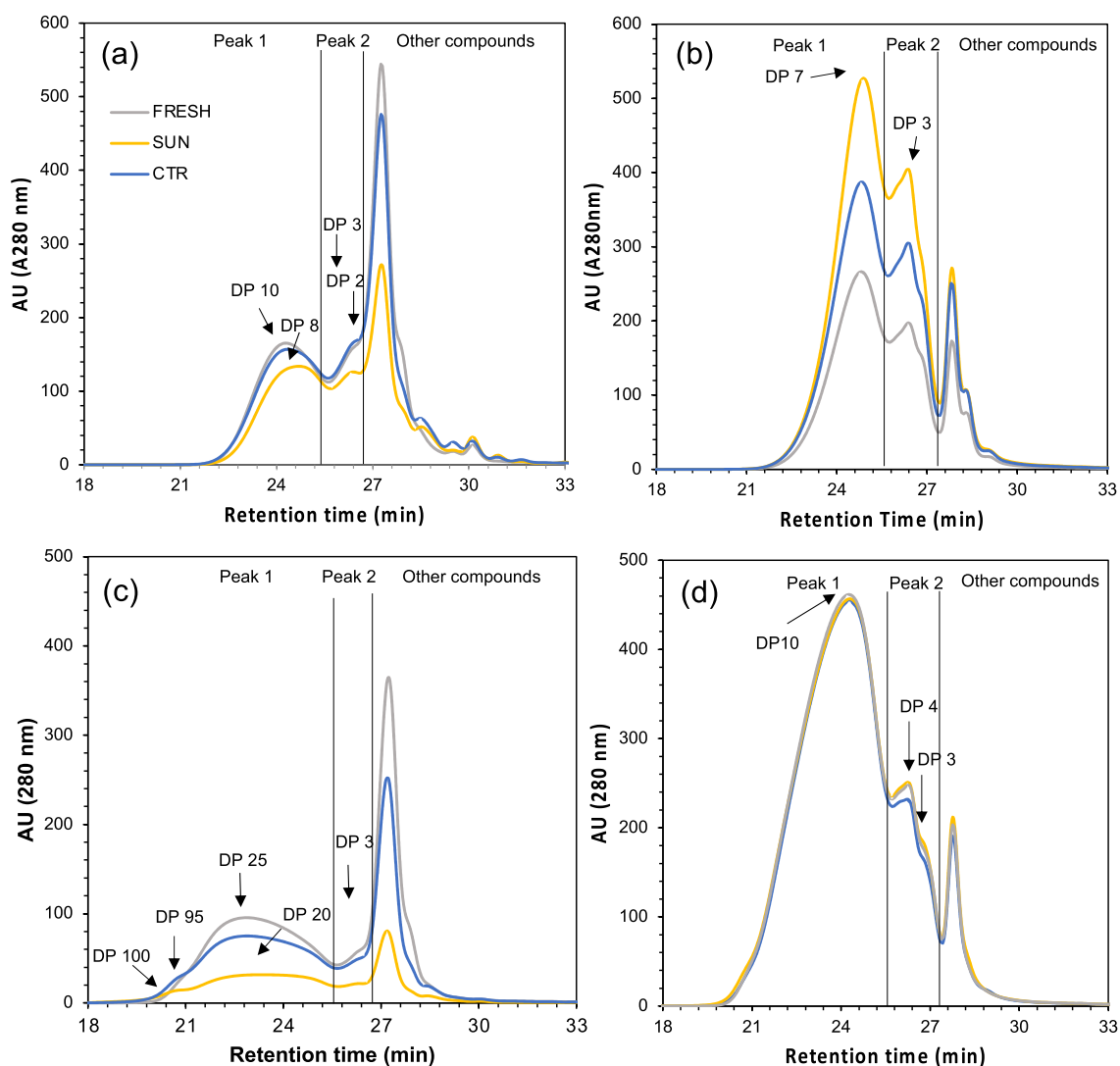


Fig. 3. – Size distribution of polymeric tannins (Peak1), oligomeric tannins (Peak2) and other polyphenol compounds such as anthocyanins or phenolic acids (Other compounds) determined by high-pressure size exclusion chromatography (HPSEC) at 280 nm. Extractable (a: skins; b: seeds) and potential (c: skins; d: seeds) HPSEC phenolic profiles for fresh (FRESH) and withered grapes under the sun (SUN) or in controlled conditions (CTR) are shown. Potential profiles of skins (c) and seeds (d) are referred to the analysis of potentially maximum extracted solutions: 150 (skins) or 100 mg (seeds) of frozen powder in 6 mL of solvent (methanol + acetone/water/formic acid); Extractable profiles are referred to the analysis of the wine-like solutions at the end of the 10 days simulated macerations of skins (a) and seeds (b). DP: degree of polymerization calculated with the calibration curve. The concentrations of potential and extractable polymers, oligomers and other compounds are shown in Table S4.

from a quantitative point of view (p-value T-test = 0.128), probably because after 96 h the diffusion rate from the SUN seeds slowed down slightly, while for CTR thinly increased. Considering the high tannin content of Aleatico seeds, particularly for low-molecular weight tannins, the duration of the maceration phase should be handled with caution in Aleatico withered grapes, preferring short macerations, especially in the case of sun-dehydration, in order to avoid unbalanced wines due to excess bitterness or astringency.

3.4. SEC Profile

The HPSEC method was performed to study the proanthocyanidin fractions mass distribution of extracts (Fig. 3). According to the SEC principle, whereby molecules of different sizes elute at different rates, the larger tannin molecules elute earlier (Kennedy & Taylor, 2003). This technique allows to also analyze the oxidized compounds, which cannot be revealed by the phloroglucinolysis or thiolysis reactions, and it is often utilized to determine the degree of polymerization (DP) of grape tannins (Bautista-Ortín, Cano-Lechuga, Ruiz-García, & Gómez-Plaza, 2014; Poncet-Legrand et al., 2010).

The HPSEC chromatograms showed three main populations: “Peak 1” related to polymeric tannins (DP > 5, according to Monagas, Gómez-Cordovés, Bartolomé, Laureano, & Ricardo da Silva, 2003) at a retention time from 20.7 to 24.9 min; “Peak 2” related to oligomers (DP > 2), eluting from 26.0 to 26.4 min; and “Other compounds”, such as anthocyanins and phenolic acids, at retention times greater than 26.5 min (Abi-Habib et al., 2021, 2022).

The HPSEC profiles were different for skins and seeds, as already observed by Abi-Habib et al. (2022). In particular, the profiles showed a majority of polymeric tannins in the seeds (“Peak 1”) and they were associated with a higher content in oligomers than in skins (Table S4). However, the average DPs of the high-molecular-weight fraction were higher for skins than for seeds (Fig. 3). Indeed, HPSEC POT phenolic profiles from skins (Fig. 3c) showed two sub-peaks within the polymeric tannin population: the first, identified at a retention time above 21 min, was characterized by a DP at its first apex of 95, 100 and 99 for FRESH, SUN and CTR samples, respectively; the second, eluted from about 23 min, presented a DP of 25, 20 and 25, respectively, for the same samples. The first sub-peaks of larger polymers were too polymerized to be extracted in wine-like conditions, probably due to the interactions with cell walls of the skins (Abi-Habib et al., 2022; Bindon et al., 2014). Consequently, the HPSEC of EXT polyphenolic profiles from skins in wine-like solutions (Fig. 3a) showed only the first peak eluted at about 24 min within the polymeric tannin population, presenting lower DPs than those estimated for the potential profile extract with strong solvents from the skins (10, 8, 10 for FRESH, SUN and CTR grapes, respectively). For seeds, the POT profiles (Fig. 3d) showed an average DP of the polymeric tannins population of 10 for all the samples studied, while the DPs of the corresponding fraction in the EXT profiles (Fig. 3b) in wine-like conditions were 7 for all the solutions, indicating that the molecular size is an important factor which affects the extraction of seeds fractions too. Indeed, the higher DP tannins are less extracted also for seeds, but to a lesser extent than for skins. This is probably due to the lower interactions with cell walls constituents and to the presence of the secondary cell walls in seeds (Boulet et al., 2023; Hanlin et al., 2010). Oligomeric tannin population (average DP = 3 for all the samples both in potential skin profiles and for extractable seeds; DP = 2–3 for extractable skins; DP = 4–3 for potential seeds), as well as polymeric population, followed the same trends described for spectrophotometric analyses: FRESH > CTR > SUN, for both potential and extractable skin profiles; FRESH=SUN=CTR for potential seed profile; SUN > CTR > FRESH, for EXT seeds profile. Indeed, in the present work, Pearson's correlation factors higher than 0.9 were obtained between the contents of tannins (polymers + oligomers fractions) estimated by HPSEC expressed as (–)-epicatechin equivalents (Table S4) and CT corresponding values (p(t)-values < 0.05 for skins and seeds CT). Instead,

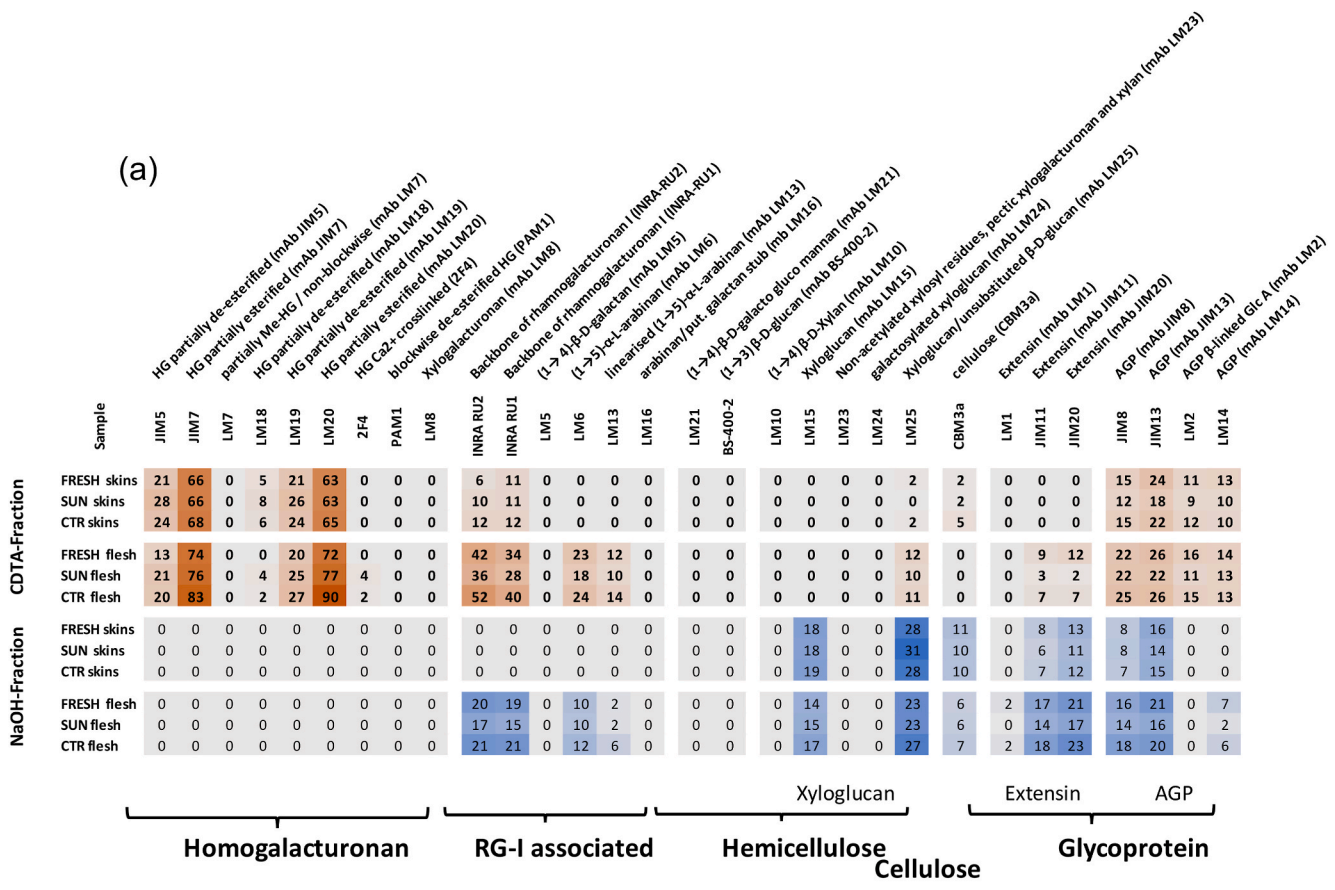
between oligomers fraction and FRV corresponding values the correlation factors resulted higher than 0.9 only for seeds (p < 0.01 for seeds FRV). Given that the FRV parameter included also monomeric flavanols, which are not comprised in HPSEC oligomer fractions, eluting with “other phenolic compounds” (from which they are indistinguishable), the FRV/CT ratios were not well correlated with the [oligomers/(oligomers + polymers)] ratios quantified by HPSEC (Pearson's correlation factors = 0.75 with p = 0.08 for skins, and 0.82 with p < 0.05 for seeds).

Interestingly, in line with the previous section, the comparison of the POT and EXT phenolic profiles showed substantial differences between those from skins and seeds: for skins (Fig. 3 a, c) the EXT profiles appeared to be the result of the combination between chemical modifications occurring during dehydration and the modified extractability; instead, seeds POT profiles were not quantitatively and qualitatively different among treatments, demonstrating that the differences shown by the extractable profiles in wine-like conditions were due to the modified extractability influenced by the withering condition, and not to metabolic modifications involving the tannins structure or their quantity. This consideration about seeds is important, since to the best of our knowledge it has never been proven. Kennedy, Matthews, and Waterhouse (2000) pointed out that the seeds coat permeability is related to the content of phenolic compounds and to their level of oxidation, which leads to a decline in their extractability. Nevertheless, as no differences were found in the present study at these levels, the observed changes in the extractability of these compounds were likely due to anatomical and histochemical tissue changes. Considering the difficulties to study seeds structure, strongly lignified, very few studies are available in the literature (Cadot, Miñana-Castelló, & Chevalier, 2006) and to our knowledge no one has been dedicated to seeds of withered grapes. Then, further specific studies need to be carried out on the potential impact of seed histochemistry modifications due to the withering process in different conditions.

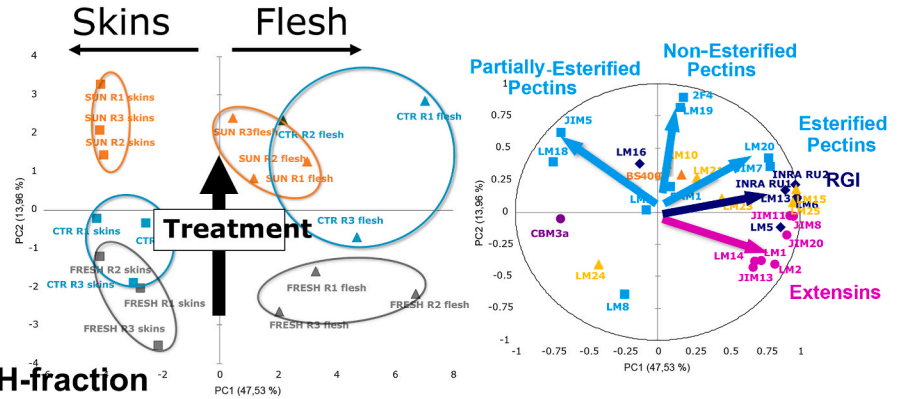
3.5. Polysaccharides of skin- and flesh-derived insoluble materials using CoMPP method

Pectin, cellulose, and hemicellulose are the three major components of the primary cell wall network (Jones-Moore, Jelley, Marangon, & Fedrizzi, 2021). The polysaccharide composition of skin and flesh cell walls was analyzed using the CoMPP method (Gao et al., 2015). The results were reported separately for the two fractions resulting from sequential extraction of the AIR material: (i) the CDTA fraction is rich in pectic polysaccharides [homogalaturonans (HG), rhamnogalaturonans I (RGI), and side chains (i.e. arabinans, galactans and arabinogalactans)], arabinogalactan-proteins (AGPs) and extensins; (ii) the NaOH fraction is rich in hemicellulosic polysaccharides (glucans/xyloglucans, mannans, xylans) and cellulose (Fig. 4). No mAb or CBMs is available to study rhamnogalaturonans of type II (RGII), while only one is available for cellulose (Abi-Habib et al., 2021).

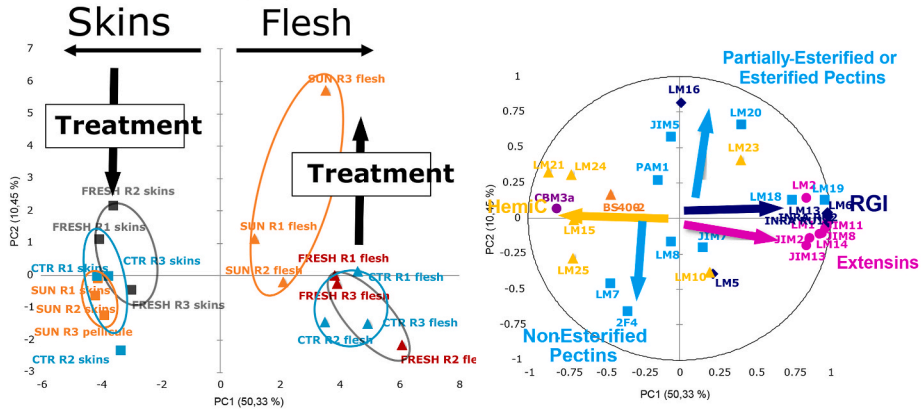
The signals reported in Fig. 4a indicate the epitope abundance accessible to the antibodies. In accordance with the literature (Abi-Habib et al., 2023; Gao, Zietsman, Vivier, & Moore, 2019), mAbs JIM7 and LM20 showed the highest signals in the pectin-rich fraction (CDTA) both in skins and flesh for all the samples studied, confirming that grape pectins are highly methyl-esterified. By examining the JIM7/JIM5 ratio (methyl de-esterified/esterified HG), among treatments SUN showed the lowest values both for skins and flesh (skins JIM7/JIM5 ratios: 3.1, 2.3, 2.8; flesh JIM7/JIM5 ratios: 5.6, 3.6, 4.15 for FRESH, SUN, and CTR, respectively), meaning a higher level of de-methylation. These results seem to be perfectly in line with the trend of skins extractability of phenolic compounds (FRESH > CTR > SUN) found in this experiment. However, Watrelot, Le Bourvellec, Imberty, & Renard (2013) pointed out that highly methylated pectins have stronger correlation with phenolic compounds, suggesting that the two phenomena appear to be only concomitant.



(b) CDTA-fraction



(c) NaOH-fraction



(caption on next page)

Fig. 4. – Comprehensive microarray polymer profiling (CoMPP) heatmap (a) representing cell wall polysaccharides and glycoproteins relative abundance of fresh grapes (FRESH), sun-withered (SUN) or withered grapes in controlled conditions (CTR). The antibodies signal intensities were read on the cyclohexane-diamino-tetraacetic acid (CDTA, pectin-rich) and NaOH (hemicellulose-rich) fractions extracted from the alcohol insoluble residue (AIR) of skins and flesh of each sample. Principal component analysis (PCA) of the variables and individual distribution regarding CDTA-fraction (b) and NaOH-fraction (c). On the PCAs, treatments (b1 and c1) are colored in grey, orange, and light blue for FRESH, SUN, and CTR, respectively; the antibodies (b2, c2) are colored as follows: in light blue those for pectin polysaccharides (HG: homogalacturonans, RG: rhamnogalacturonans and side chains: arabinans, galactans and arabinogalactans); in yellow the antibodies for hemicellulosic polysaccharides (mannans, glucan/xyloglucans, and xylans); in pink those for glycoproteins (AGP: arabinogalactan-Proteins, and extensins). The antibodies used and their functions are described in detail in [Table S1](#).

Indeed, HG de-methylation releases COO^- functions allowing the formation of egg-boxes through Ca^{2+} bridges, which play an important role in the structural features of the cell walls, forming a very rigid gel, which can hinder the release of compounds, modifying the cell wall porosity and the strength of intracellular adhesion (Basak & Bandyopadhyay, 2014). The changes in the cell wall structure by de-esterification and de-polymerization, together with the possible formation of new Ca-bridges could reduce tannin extractability due to their encapsulation in the modified gel network (Hanlin et al., 2010). This pattern is probably a metabolic strategy to reduce the loss of water from grape berries during dehydration. It is noticeable that in the present study, the 2F4 signal for calcium egg-boxes is higher for withered grapes (SUN > CTR) only in flesh. Nevertheless, the absence of these signals in the skins could be due to the extraction fractions (CDTA and NaOH) which are not strong enough to reveal them (Gao et al., 2015), as the polysaccharides are more strongly held in the skins than in the flesh cell walls matrix (Vidal, Williams, O'neill, & Pellerin, 2001).

The higher de-methylation of withered samples compared to FRESH observed in the present study was in accordance with the increased activity of pectin methyl esterase (PME) found in literature during dehydration (Vincenzi et al., 2012; Zoccatelli et al., 2013). The higher temperatures of SUN withering than CTR conditions may have increased the PME activity, explaining the great difference between the two dehydration modalities (Coletta et al., 2019). Skins resulted higher de-esterified than flesh, in accordance with the findings of Fasoli et al. (2019), who highlighted a higher level of de-esterification in the external layers of the skins compared with the internals. Moreover, Zoccatelli et al. (2013) demonstrated that the coordination of PME and polygalacturonase (PG) activity is variety-dependent: they led to the degradation of skins pectins only for one of the three varieties studied (Corvina), whereas in cv. Oseleta and Sangiovese the activity of the two enzymes was uncoupled throughout dehydration and it was supposed to serve a different role. Indeed, the increase of pH (higher for sun than CTR) and the higher availability of Ca^{2+} ions due to the intense cell wall degradation of withered grapes are known to inhibit the PG activity in withered grapes, to a greater extent for SUN samples (Botondi, Lodola, & Mencarelli, 2011). This fact could make significant only the effect of the increased de-methylation, which probably determined the lowest extractability of anthocyanins and polyphenols from SUN skins. The high amounts of HG, RGI, and AGPs detected in the CDTA fractions could confirm the supposed low activity of PG, as Kuhlman, Hansen, Jørgensen, du Toit, and Moore (2022) demonstrated a complete or significant reduction of these signals after its action. Instead, the NaOH extraction (hemicellulose-rich fraction) showed strong signals of xyloglucans (mAbs LM15 and LM25), cellulose (CBM3a), as well as glycoproteins (mAbs JIM11 and JIM20 as extensins, and JIM8 and JIM13 as AGPs). In SUN withered grapes, a decline in signals of extensins epitopes was found (mAbs LM1 for flesh, and JIM 11, JIM20 for both skins and flesh), together with a decline in AGPs signals (mAbs JIM8, JIM13 for skins and flesh, and LM14 only for the flesh). These findings agree with the observations of Gao et al. (2021) on Syrah overripe grapes. These authors attributed the degradation of glycoproteins in the NaOH fraction to a degradation of the pectin extension network due to heat, sunlight exposure, and water deficit stress.

To better understand the differences among treatments and tissues, a principal component analysis (PCA) was performed separately for each fraction (Fig. 4 b-c). For both CDTA and NaOH, the horizontal axis

reproduced the type of tissue studied (skins or flesh), while the vertical axis (PC2) the differences among treatments. Regarding CDTA-fraction (Fig. 4b), principal component 1 (PC1) accounted for 47.53% of the explained variance, whereas principal component 2 (PC2) explained 13.96%, with a total explained variance by the first two components of 61.49%. Skins and flesh were separated on PC1 axis for the higher presence of RGI hairy regions and extensins/AGPs in the Aleatico flesh than in skins for all the treatments studied. In accordance with these findings, Vidal et al. (2001), studying the composition of polysaccharides from different tissues (skins and flesh) of grapes cv. Grenache blanc, pointed out that 80% of grape AGPs come from the flesh, whereas, differently from what observed for Aleatico, RGI were present in both tissues in comparable amounts. Indeed, Ortega-Regules, Ros-García, Bautista-Ortín, López-Roca, and Gómez-Plaza (2008) demonstrated that the composition and total sugar content of cell walls are variety-dependent. Comparing treatments, CTR replicates were more similar to FRESH in the skins and to SUN in the flesh. PC2 separated FRESH, SUN, and CTR treatments based on their changes in pectin HG zones. In particular, the withering modalities studied (SUN and CTR) differed for the HG zones of partially esterified pectins (JIM5 and LM18) for the skins, and with a lesser extent of esterified pectins for the flesh (JIM7 and LM20). Regarding the NaOH fraction (Fig. 4c), the PCA showed a total explained variance of 60.78% (50.33 and 10.45 for PC1 and PC2, respectively). Skins and flesh were separated on the axis PC1 because the higher hemicellulose detected in the skins, whereas pulps were richer in pectins RGI hairy regions and extensins/AGPs. On the contrary to what was observed in the CDTA-PCA, CTR resulted more like SUN in the skins and to FRESH in the flesh. Among treatments (PG2 vertical axis), FRESH showed lower de-esterified HG (LM7 and 2F4) than withered samples for the skins, while for the flesh SUN presented higher contents of HG partially esterified (JIM5) or totally esterified (LM20) than other samples.

3.6. Sugar composition determined by GC analyses

To complete the study of the cell wall polysaccharides modifications in cv. Aleatico grapes subjected to different withering conditions, the chemical composition of polymers was also analyzed with the classical chemical analyses, which are based on the determination of their monosaccharide constitutive units after depolymerization steps. Indeed, some studies have recently been oriented towards the combination of the composition determined by chemical analyses coupled with the CoMPP immunochemical analysis, which can provide new awareness on the conditions of cell walls polymers (Boulet et al., 2023). TMS was used to assess the qualitative profile of neutral and acidic sugars, providing the molar ratio of the monosaccharides composition of skins and flesh AIS cell wall material (Fig. 5). Instead, the quantification (mg/g AIS) of single monosaccharides was performed by GC analysis of alditol acetates (pectins and hemicelluloses) and alditol acetates after Saeman hydrolysis (pectins; hemicelluloses and cellulose). The results are reported in Table S5. However, from the comparison between the glucose detected by alditol acetates and Saeman methods, it emerged that the Saeman hydrolysis worked for pulps and fresh skins, but probably failed to completely hydrolyse the cellulose in the withered skins as alditols acetates showed higher glucose than Saeman method for these samples. The reasons for this difficulty are probably due to morphological and chemical alterations that occur during withering (Fasoli et al., 2019) and

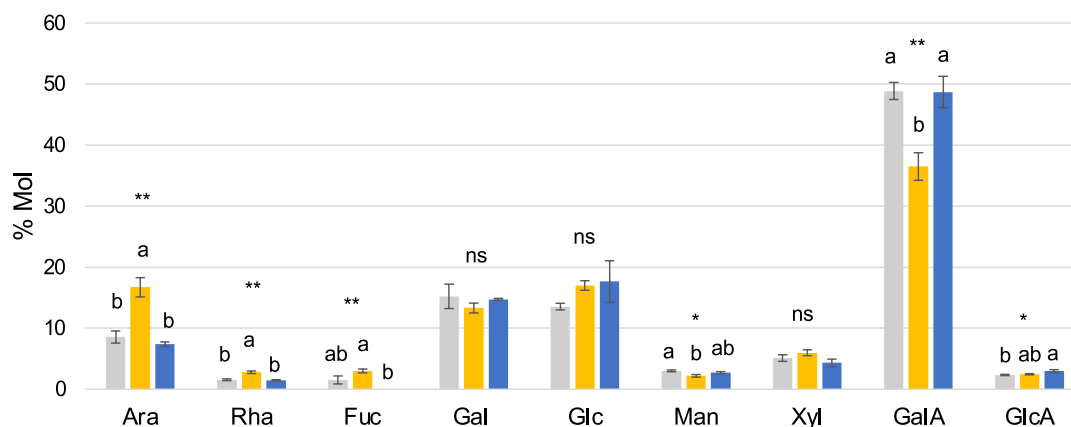
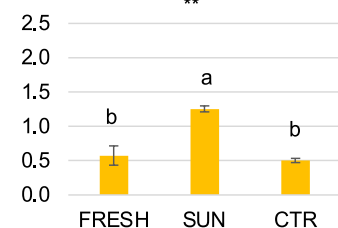
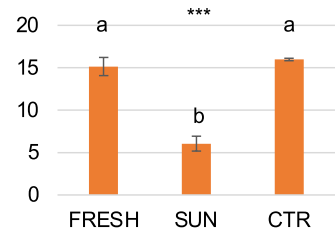
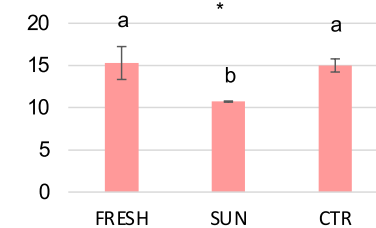
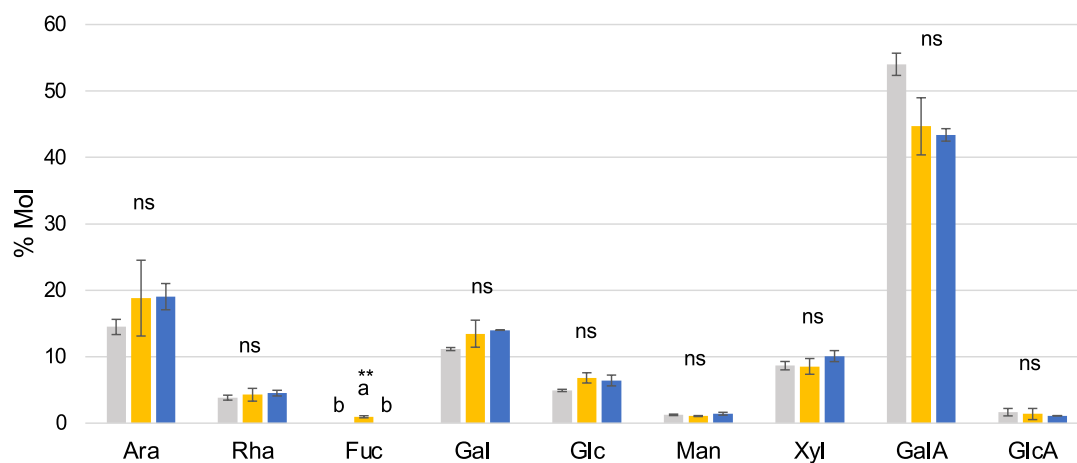
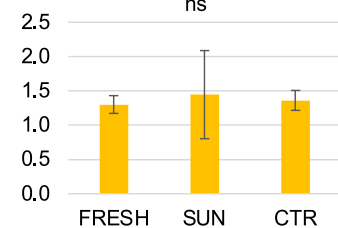
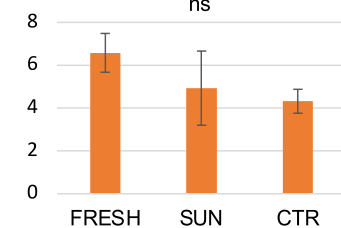
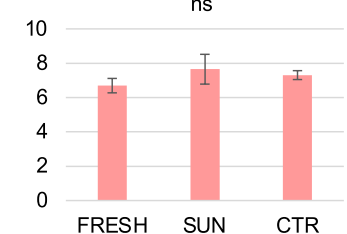
(a) Skins**(a1) Ara/Gal****(a2) (GalA-Rha)/2Rha****(a3) (Ara + Gal)/Rha****(b) Flesh****(b1) Ara/Gal****(b2) (GalA-Rha)/2Rha****(b3) (Ara + Gal)/Rha**

Fig. 5. – Molar ratio of glycosyl-residue of AIs polysaccharides of Aleatico skins (a) and pulps (b) of the three modalities studied (FRESH (grey): fresh grapes; SUN (yellow): sun-withered grapes; CTR (blue): withered grapes in controlled conditions) obtained with the TMS analysis. Ara: arabinose; Rha: rhamnose; Fuc: fucose; Gal: galactose; Glc: glucose; Man: mannose; Xyl: xylose; GalA: galacturonic acid; GlcA: glucuronic acid.

particularly to the reorganization of the gel network structures, as CoMPP results highlighted.

Galacturonic acid (from pectins) and glucose (from cellulose and hemicellulose) were the major AISs compounds in skins (Fig. 5a), accounting from 36 to 49% and 14–18% of analyzed AISs, respectively. Also, arabinose and galactose (from pectins rhamnogalacturonan side chains) showed high molar ratios (9–17% and 13–15%). Nevertheless, the significantly higher molar ratios of arabinose, rhamnose, and fucose found in SUN skins were due to the most remarkable decrease of all the other sugars and not to their real increase in quantity, as shown in Table S5 by the results expressed in mg/g AIS obtained by GC of alditol acetates and by Seaman hydrolysis. On the contrary, significantly lower percentages of galacturonic acid and mannose (hemicellulose) were found in SUN with respect to other treatments. The only significant difference between FRESH and CTR grape skins molar ratio of neutral sugars was detected for glucuronic acid, which was significantly higher for CTR than FRESH, whereas SUN was intermediate between the two values (2.3, 2.5 and 3.0% for FRESH, SUN and CTR).

The calculation of different specific ratios of sugars (Fig. 5 a) allowed to estimate the relative importance of polysaccharides to better understand their structural modifications: arabinose/galactose (Ara/Gal), (galacturonic acid – rhamnose)/2rhamnose acid [(GalA-Rha)/(2*Rha)], and (arabinose + galactose)/rhamnose [(Ara + Gal)/Rha] (Apolinar-Valiente et al., 2018; Huang et al., 2017). For all the specific ratios, SUN resulted significantly different compared with CTR and FRESH, whereas FRESH and CTR were not statistically different each other. In particular, the Ara/Gal ratio is characteristic of the PRAG-like structures (polysaccharides rich in arabinose and galactose). Its modification detected in AISs cell wall skins (0.57, 1.25, and 0.50 for FRESH, SUN and CTR, respectively) could be due to the degradation of AGPs observed in the CoMPP hemicellulose-rich fraction (Doco, Williams, & Cheynier, 2007). Moreover, the higher [(GalA-Rha)/(2*Rha)], ratio of SUN skins (6.05 for SUN vs 15.15 and 15.99 for CTR and FRESH, respectively) indicates that SUN cell walls insoluble pectins were characterised by higher relative amounts of RG than HG with respect to other samples, consistently to the CoMPP results (Fig. 4). In addition, since most of arabinose and galactose are associated with pectin hairy regions, the lower (arabinose + galactose)/rhamnose ratio calculated for SUN skins (15.30, 10.73 and 15.01 for FRESH, SUN, and CTR, respectively) indicates that they were characterized by RG-like backbone structures which carry shorter neutral chains than FRESH and CTR. Therefore, the withering process strongly affected the neutral sugar composition of skin AISs cell walls, particularly when the grapes were dehydrated in natural conditions under the sun. However, our findings regarding the relationship between the extractability of phenolic compounds and skin cell wall composition seem to be in contrast with the correlations found by other authors, who recently studied their extractability linked with polysaccharides composition in fresh grapes (Abi-Habib et al., 2022, 2023; Boulet et al., 2023). It is possible that the supposed modifications of gel network structures in withered grapes physically influence the extractability of phenolic compounds from withered skins differently to fresh grapes. However, as Boulet et al. (2023) concluded, predicting the extraction of anthocyanins and tannins in wine from the grapes remains a challenge, and further studies aimed at a polysaccharides-polyphenols characterization could help in this direction.

As regards grape flesh (Fig. 4b), it showed on average lower percentage of mannose and glucose than skins, confirming the lower presence of hemicellulose in flesh AISs cell wall of cv. Aleatico with respect to the skins, in accordance with CoMPP results. Instead, galacturonic acid is highly represented (more than 40% in all the samples), indicating an important quantity of pectins in Aleatico flesh. Among treatments, however, the withering process did not significantly affect the composition of the flesh, regardless of the conditions applied (Fig. 4b), except for fucose, which is a specific component of RGII (Doco et al., 2007) and to a lesser extent xyloglucans (Doco, Williams, Pauly, O'Neill, & Pellerin, 2003).

4. Conclusion

The characterization of flesh and skin AISs cell wall polysaccharide of Aleatico cv. through chemical and immunochemical approaches confirmed that AISs composition is a varietal-dependent feature. The results showed that withering process strongly affected the neutral sugar composition of skins AIS cell walls, particularly when the grapes were dehydrated in natural conditions under the sun, especially at the level of pectin chains and de-esterification. Instead, grape flesh polysaccharides undergo less marked changes.

At the end of the withering, SUN grapes showed the highest pH and the lowest acidity values, whereas these parameters were better preserved in CTR conditions. SUN skin macerating solutions experienced the lowest contents of anthocyanins and tannins, both for oligomers and polymers. SEC profiles highlighted a higher level of tannins polymerization in withered skins compared to FRESH, especially for SUN. However, high-polymerized tannins (DP > 10) were too large to be extracted from the skins, leading to a lower DP of the high-polymerized fraction in SUN wine-like extracts compared with other samples. Indeed, the extractability of phenolic compounds decreased in skins after withering, with a greater extent for SUN than CTR, except for the low-molecular tannins (FRV), which showed no significant differences in extractability among treatments, although they were involved in other chemical reactions (oxidation, polymerization).

The extractable phenolic profiles of skins in wine-like conditions were determined by the different extraction yields (FRESH > CTR > SUN) probably caused by the cell wall modifications, combined with a loss of compounds by oxidation and other chemical reactions, which was overcome by the concentration effect for withering under controlled conditions, but not always for SUN grapes, due to the higher degradation caused by higher temperatures and sunlight exposure. The extraction kinetics of anthocyanins in both the withering modalities were slower than those of fresh grapes, according to the greater skin thickness (Sp_{sk}) of withered grapes compared to the fresh, which did not show significant differences between the dehydration conditions.

As opposed to the skins, the extractability of phenolics and tannins from seeds increased after withering, again with a greater extent for SUN grapes (SUN > CTR > FRESH). For the first time, it was clearly demonstrated that seed total phenolic profiles were not quantitatively and qualitatively affected by the withering from a chemical point of view. Therefore, the differences shown by the extractable profiles in wine-like conditions were due to a modified extractability as consequence of the different withering conditions and not to chemical modifications of phenolic compounds during the withering process. Given the difficulty of studying seed tissues, specific studies are necessary to understand the physical causes of the differences observed in extractability, probably due to the softening of seeds withered tissues. Also, in the case of seeds, at the end of the 10-days of simulated macerations, the phenolic profile of CTR extracts was more similar to FRESH samples than SUN.

Consequently, the differences observed between the two withering conditions studied for different tissues were substantial: SUN grapes contained fewer polyphenols from the skins than FRESH and CTR and the highest phenolics from seeds. This information is particularly interesting when choosing maceration strategies: on one hand, to better preserve the compounds of the skins, which are fewer and extracted more slowly in withered grapes than fresh grapes, particularly in the case of high withering temperatures and sunlight exposure conditions; on the other hand, to regulate the extraction of phenolic compounds from grape seeds, especially as regards tannins. Indeed, the faster seeds extraction and the higher extraction yields observed for polyphenols suggest reducing the maceration days to produce more balanced wines or modulating them according to the desired oenological objective.

The findings provide new awareness on the extractability of phenolic compounds from grapes subjected to different withering conditions, in perspective with cell wall polysaccharides and mechanical properties

modifications, helping winemakers to choose the best maceration strategy to valorize the varietal characteristics of withered grapes.

Funding

This publication is part of the project NODES which has received funding from the MUR – M4C2 1.5 of PNRR with grant agreement no. ECS00000036.

CRediT authorship contribution statement

Giulia Scalzini: Conceptualization, Data curation, Formal analysis, Investigation, Writing – original draft, Visualization. **Aude Vernhet:** Conceptualization, Methodology, Supervision, Writing – review & editing, Investigation, Project administration, Validation. **Stéphanie Carillo:** Data curation, Formal analysis, Methodology, Resources, Writing – review & editing. **Stéphanie Roi:** Data curation, Formal analysis, Methodology, Resources, Writing – review & editing. **Frédéric Véran:** Data curation, Formal analysis, Methodology, Resources, Writing – review & editing. **Bodil Jørgensen:** Data curation, Formal analysis, Investigation, Methodology, Resources, Writing – review & editing. **Jeanett Hansen:** Data curation, Formal analysis, Methodology, Writing – review & editing. **Simone Giacosa:** Conceptualization, Formal analysis, Methodology, Project administration, Validation, Writing – review & editing. **Susana Río Segade:** Conceptualization, Investigation, Supervision, Writing – review & editing. **Maria Alesandra Paissoni:** Conceptualization, Formal analysis, Methodology, Writing – review & editing. **Thierry Doco:** Conceptualization, Investigation, Methodology, Project administration, Supervision, Validation, Visualization, Writing – review & editing. **Luca Rolle:** Conceptualization, Funding acquisition, Project administration, Supervision, Writing – review & editing. **Céline Poncet-Legrand:** Conceptualization, Investigation, Methodology, Project administration, Supervision, Validation, Writing – review & editing.

Declaration of competing interest

The authors declare that they have no known competing financial interests or personal relationships that could have appeared to influence the work reported in this paper.

Data availability

No data was used for the research described in the article.

Acknowledgements

Giulia Scalzini would like to thank all the authors for their support and contributions for this research.

Appendix A. Supplementary data

Supplementary data to this article can be found online at <https://doi.org/10.1016/j.foodhyd.2023.109605>.

References

- Abi-Habib, E., Poncet-Legrand, C., Roi, S., Carrillo, S., Doco, T., & Vernhet, A. (2021). Impact of grape variety, berry maturity and size on the extractability of skin polyphenols during model wine-like maceration experiments. *Journal of the Science of Food and Agriculture*, 101(8), 3257–3269. <https://doi.org/10.1002/jsfa.10955>
- Abi-Habib, E., Vernhet, A., Roi, S., Carrillo, S., Jørgensen, B., Hansen, J., et al. (2022). Impact of the variety on the adsorption of anthocyanins and tannins on grape flesh cell walls. *Journal of the Science of Food and Agriculture*, 102(8), 3379–3392. <https://doi.org/10.1002/jsfa.11685>
- Abi-Habib, E., Vernhet, A., Roi, S., Carrillo, S., Veran, F., Ducasse, M. A., et al. (2023). Diffusion of phenolic compounds during a model maceration in winemaking: Role of

- flesh and seeds. *Journal of the Science of Food and Agriculture*, 103(4), 2004–2013. <https://doi.org/10.1002/jsfa.12331>
- Anderson, K., & Aryal, N. R. (2013). *Which winegrape varieties are grown where? A global empirical picture*. Australia: University of Adelaide Press. <http://library.oapen.org/handle/20.500.12657/33146>.
- Apolinar-Valiente, R., Romero-Cascales, I., Gómez-Plaza, E., López-Roca, J. M., & Ros-García, J. M. (2015). The composition of cell walls from grape marcs is affected by grape origin and enological technique. *Food Chemistry*, 167, 370–377. <https://doi.org/10.1016/j.foodchem.2014.07.030>
- Apolinar-Valiente, R., Ruiz-García, Y., Williams, P., Gil-Muñoz, R., Gómez-Plaza, E., & Doco, T. (2018). Preharvest application of elicitors to Monastrell grapes: Impact on wine polysaccharide and oligosaccharide composition. *Journal of Agricultural and Food Chemistry*, 66(42), 11151–11157. <https://doi.org/10.1021/acs.jafc.8b05231>
- Barnuud, N. N., Zerihun, A., Gibberd, M., & Bates, B. (2014). Berry composition and climate: Responses and empirical models. *International Journal of Biometeorology*, 58(6), 1207–1223. <https://doi.org/10.1007/s00484-013-0715-2>
- Basak, R., & Bandyopadhyay, R. (2014). Formation and rupture of Ca²⁺ induced pectin biopolymer gels. *Soft Matter*, 10(37), 7225–7233. <https://doi.org/10.1039/c4m00748d>
- Bautista-Ortín, A. B., Cano-Lechuga, M., Ruiz-García, Y., & Gómez-Plaza, E. (2014). Interactions between grape skin cell wall material and commercial enological tannins. Practical implications. *Food Chemistry*, 152, 558–565. <https://doi.org/10.1016/j.foodchem.2013.12.009>
- Bellincontro, A., Fardelli, A., De Santis, D., Botondi, R., & Mencarelli, F. (2006). Postharvest ethylene and 1-MCP treatments both affect phenols, anthocyanins, and aromatic quality of Aleatico grapes and wine. *Australian Journal of Grape and Wine Research*, 12(2), 141–149. <https://doi.org/10.1111/j.1755-0238.2006.tb00054.x>
- Bellincontro, A., Matarese, F., D'Onofrio, C., Accordini, D., Tosi, E., & Mencarelli, F. (2016). Management of postharvest grape withering to optimise the aroma of the final wine: A case study on amarone. *Food Chemistry*, 213, 378–387. <https://doi.org/10.1016/j.foodchem.2016.06.098>
- Bergqvist, J., Dokoozlian, N., & Ebisuda, N. (2001). Sunlight exposure and temperature effects on berry growth and composition of cabernet sauvignon and grenache in the central san joaquin valley of California. *American Journal of Enology and Viticulture*, 52(1), 1–7. <https://doi.org/10.5344/ajev.2001.52.1.1>
- Bindon, K. A., Madani, S. H., Pendleton, P., Smith, P. A., & Kennedy, J. A. (2014). Factors affecting skin tannin extractability in ripening grapes. *Journal of Agricultural and Food Chemistry*, 62(5), 1130–1141. <https://doi.org/10.1021/jf4050606>
- Bonghi, C., Rizzini, F. M., Gambuti, A., Moio, L., Chkaban, L., & Tonutti, P. (2012). Phenol compound metabolism and gene expression in the skin of wine grape (*Vitis vinifera* L.) berries subjected to partial postharvest dehydration. *Postharvest Biology and Technology*, 67, 102–109. <https://doi.org/10.1016/j.postharvbio.2012.01.002>
- Botondi, R., Lodola, L., & Mencarelli, F. (2011). Postharvest ethylene treatment affects berry dehydration, polyphenol and anthocyanin content by increasing the activity of cell wall enzymes in Aleatico wine grape. *European Food Research and Technology*, 232(4), 679–685. <https://doi.org/10.1007/s00217-011-1437-5>
- Boulet, J. C., Abi-Habib, E., Carrillo, S., Roi, S., Veran, F., Verbaere, A., et al. (2023). Focus on the relationships between the cell wall composition in the extraction of anthocyanins and tannins from grape berries. *Food Chemistry*, 406, Article 135023. <https://doi.org/10.1016/j.foodchem.2022.135023>
- Boulton, R. (1980). The general relationship between potassium, sodium and pH in grape juice and wine. *American Journal of Enology and Viticulture*, 31(2), 182–186.
- Busse-Valverde, N., Gomez-Plaza, E., Lopez-Roca, J. M., Gil-Munoz, R., & Bautista-Ortín, A. B. (2011). The extraction of anthocyanins and proanthocyanidins from grapes to wine during fermentative maceration is affected by the enological technique. *Journal of Agricultural and Food Chemistry*, 59(10), 5450–5455. <https://doi.org/10.1021/jf2002188>
- Cadot, Y., Miñana-Castelló, M. T., & Chevalier, M. (2006). Anatomical, histological, and histochemical changes in grape seeds from *Vitis vinifera* L. cv Cabernet franc during fruit development. *Journal of Agricultural and Food Chemistry*, 54(24), 9206–9215. <https://doi.org/10.1021/jf061326f>
- Canals, R., Llaudy, M. C., Valls, J., Canals, J. M., & Zamora, F. (2005). Influence of ethanol concentration on the extraction of color and phenolic compounds from the skin and seeds of Tempranillo grapes at different stages of ripening. *Journal of Agricultural and Food Chemistry*, 53(10), 4019–4025. <https://doi.org/10.1021/jf047872v>
- Centioni, L., Tiberi, D., Pietromarchi, P., Bellincontro, A., & Mencarelli, F. (2014). Effect of postharvest dehydration on content of volatile organic compounds in the epicarp of Cesanese grape berry. *American Journal of Enology and Viticulture*, 65(3), 333–340. <https://doi.org/10.5344/ajev.2014.13126>
- Cheng, H. D., Jiang, X. H., Sun, Y., & Wang, J. (2001). Color image segmentation: Advances and prospects. *Pattern Recognition*, 34(12), 2259–2281. [https://doi.org/10.1016/S0031-3203\(00\)00149-7](https://doi.org/10.1016/S0031-3203(00)00149-7)
- Cheyrier, V., Basire, N., & Rigaud, J. (1989). Mechanism of trans-caffeoyltartaric acid and catechin oxidation in model solutions containing grape polyphenoloxidase. *Journal of Agricultural and Food Chemistry*, 37(4), 1069–1071. <https://hal.inrae.fr/hal-02722125>.
- Cheyrier, V., Duenas-Paton, M., Salas, E., Maury, C., Souquet, J. M., Sarni-Manchado, P., et al. (2006). Structure and properties of wine pigments and tannins. *American Journal of Enology and Viticulture*, 57(3), 298–305. <https://doi.org/10.5344/ajev.2006.57.3.298>
- Chira, K., Schmauch, G., Saucier, C., Fabre, S., & Teissedre, P. L. (2009). Grape variety effect on proanthocyanidin composition and sensory perception of skin and seed tannin extracts from Bordeaux wine grapes (Cabernet Sauvignon and Merlot) for two consecutive vintages (2006 and 2007). *Journal of Agricultural and Food Chemistry*, 57(2), 545–553. <https://doi.org/10.1021/jf802301g>

- Río Segade, S., Paissoni, M. A., Giacosa, S., Bautista-Ortín, A. B., Gómez-Plaza, E., Gerbi, V., et al. (2019a). Winegrapes dehydration under ozone-enriched atmosphere: Influence on berry skin phenols release, cell wall composition and mechanical properties. *Food Chemistry*, 271, 673–684. <https://doi.org/10.1016/j.foodchem.2018.07.218>
- Río Segade, S., Paissoni, M. A., Vilanova, M., Gerbi, V., Rolle, L., & Giacosa, S. (2019b). Phenolic composition influences the effectiveness of fining agents in vegan-friendly red wine production. *Molecules*, 25(1), 120. <https://doi.org/10.3390/molecules25010120>
- Río Segade, S., Torchio, F., Gerbi, V., Quijada-Morín, N., García-Estévez, I., Giacosa, S., et al. (2016). Impact of postharvest dehydration process of winegrapes on mechanical and acoustic properties of the seeds and their relationship with flavanol extraction during simulated maceration. *Food Chemistry*, 199, 893–901. <https://doi.org/10.1016/j.foodchem.2015.12.072>
- Rolle, L., Giacosa, S., Río Segade, S., Ferrarini, R., Torchio, F., & Gerbi, V. (2013). Influence of different thermohygrometric conditions on changes in instrumental texture properties and phenolic composition during postharvest withering of 'Corvina' winegrapes (*Vitis vinifera* L.). *Drying Technology*, 31(5), 549–564. <https://doi.org/10.1080/07373937.2012.745092>
- Rolle, L., Torchio, F., Giacosa, S., & Gerbi, V. (2009). Modifications of mechanical characteristics and phenolic composition in berry skins and seeds of Mondeuse winegrapes throughout the on-vine drying process. *Journal of the Science of Food and Agriculture*, 89(11), 1973–1980. <https://doi.org/10.1002/jsfa.3686>
- Rolle, L., Torchio, F., Zeppa, G., & Gerbi, V. (2008). Anthocyanin extractability assessment of grape skins by texture analysis. *Oeno One*, 42(3), 157–162. <https://doi.org/10.20870/oeno-one.2008.42.3.819>
- Saeman, J. F., Moore, W. E., Mitchell, R. L., & Millett, M. A. (1954). Techniques for the determination of pulp constituents by quantitative paper chromatography. *The Journal of the Technical Association of the Pulp and Paper Industry*, 37(8), 336–343.
- Sanmartin, C., Modesti, M., Venturi, F., Brizzolara, S., Mencarelli, F., & Bellincontro, A. (2021). Postharvest water loss of wine grape: When, what and why. *Metabolites*, 11(5), 318. <https://doi.org/10.3390/metabo11050318>
- Sarneckis, C. J., Damberg, R. G., Jones, P., Mercurio, M., Herderich, M. J., & Smith, P. A. (2006). Quantification of condensed tannins by precipitation with methyl cellulose: Development and validation of an optimised tool for grape and wine analysis. *Australian Journal of Grape and Wine Research*, 12(1), 39–49. <https://doi.org/10.1111/j.1755-0238.2006.tb00042.x>
- Scalzini, G., Giacosa, S., Río Segade, S., Paissoni, M. A., & Rolle, L. (2021). Effect of withering process on the evolution of phenolic acids in winegrapes: A systematic review. *Trends in Food Science & Technology*, 116, 545–558. <https://doi.org/10.1016/j.tifs.2021.08.004>
- Scalzini, G., López-Prieto, A., Paissoni, M. A., Englezos, V., Giacosa, S., Rolle, L., et al. (2020). Can a corn-derived biosurfactant improve colour traits of wine? First insight on its application during winegrape skin maceration versus oenological tannins. *Foods*, 9(12), 1747. <https://doi.org/10.3390/foods9121747>
- Spayd, S. E., Tarara, J. M., Mee, D. L., & Ferguson, J. C. (2002). Separation of sunlight and temperature effects on the composition of *Vitis vinifera* cv. Merlot berries. *American journal of enology and viticulture. American Journal of Enology and Viticulture*, 53(3), 171–182. <https://doi.org/10.5344/ajev.2002.53.3.171>, 53, 171–182.
- Sternad Lemut, M., Sivilotti, P., Franceschi, P., Wehrens, R., & Vrhovsek, U. (2013). Use of metabolic profiling to study grape skin polyphenol behavior as a result of canopy microclimate manipulation in a 'Pinot noir' vineyard. *Journal of Agricultural and Food Chemistry*, 61(37), 8976–8986. <https://doi.org/10.1021/jf4030757>
- Toffali, K., Zamboni, A., Anesi, A., Stocchero, M., Pezzotti, M., Levi, M., et al. (2011). Novel aspects of grape berry ripening and post-harvest withering revealed by untargeted LC-ESI-MS metabolomics analysis. *Metabolomics*, 7(3), 424–436. <https://doi.org/10.1007/s11306-010-0259-y>
- Torchio, F., Cagnasso, E., Gerbi, V., & Rolle, L. (2010). Mechanical properties, phenolic composition and extractability indices of Barbera grapes of different soluble solids contents from several growing areas. *Analytica Chimica Acta*, 660(1–2), 183–189. <https://doi.org/10.1016/j.aca.2009.10.017>
- Tuccio, L. (2011). *Aleatico grapevine characterization: Physiological and molecular responses to different water regimes*. Italy: University of Pisa. PhD Thesis.
- Vernhet, A., Carrillo, S., & Poncet-Legrand, C. (2014). Condensed tannin changes induced by autoxidation: Effect of the initial degree of polymerization and concentration. *Journal of Agricultural and Food Chemistry*, 62(31), 7833–7842. <https://doi.org/10.1021/jf501441j>
- Vernhet, A., Carrillo, S., Rattier, A., Verbaere, A., Cheynier, V., & Nguela, J. M. (2020). Fate of anthocyanins and proanthocyanidins during the alcoholic fermentation of thermovinified red musts by different *Saccharomyces cerevisiae* strains. *Journal of Agricultural and Food Chemistry*, 68(11), 3615–3625. <https://doi.org/10.1021/acs.jafc.0c00413>
- Vidal, S., Williams, P., O'neill, M. A., & Pellerin, P. (2001). Polysaccharides from grape berry cell walls. Part I: Tissue distribution and structural characterization of the pectic polysaccharides. *Carbohydrate Polymers*, 45(4), 315–323. [https://doi.org/10.1016/S0144-8617\(00\)00285-X](https://doi.org/10.1016/S0144-8617(00)00285-X)
- Vincenzi, S., Tolin, S., Coccolin, L., Rantsiou, K., Curioni, A., & Rolle, L. (2012). Proteins and enzymatic activities in Erbaluce grape berries with different response to the withering process. *Analytica Chimica Acta*, 732, 130–136. <https://doi.org/10.1016/j.aca.2011.11.058>
- Watrelet, A. A., Le Bourvellec, C., Imbert, A., & Renard, C. M. G. C. (2013). Interactions between pectic compounds and procyanidins are influenced by methylation degree and chain length. *Biomacromolecules*, 14(3), 709–718. <https://doi.org/10.1021/bm301796y>
- Zenoni, S., Fasoli, M., Guzzo, F., Dal Santo, S., Amato, A., Anesi, A., et al. (2016). Disclosing the molecular basis of the postharvest life of berry in different grapevine genotypes. *Plant Physiology*, 172(3), 1821–1843. <https://doi.org/10.1104/pp.16.00865>
- Zoccatelli, G., Zenoni, S., Savoi, S., Dal Santo, S., Tononi, P., Zandonà, V., et al. (2013). Skin pectin metabolism during the postharvest dehydration of berries from three distinct grapevine cultivars. *Australian Journal of Grape and Wine Research*, 19(2), 171–179. <https://doi.org/10.1111/ajgw.12014>